ISSN 1810-0384

ADVANCES IN ELECTROMETALLURGY

No. 4 Volume 9 2011

CAMBRIDGE INTERNATIONAL SCIENCE PUBLISHING

Advances in Electrometallurgy is a cover-to-cover English translation of *Sovremennaya Elektrometallurgiya*, published four times a year by International Association 'Welding' at the E.O. Paton Electric Welding Institute, National Academy of Sciences of Ukraine, 11 Bozhenko Street, 03680 Kyiv, Ukraine

Published by

Cambridge International Science Publishing Ltd
7 Meadow Walk, Great Abington, Cambridge CB21 6AZ, England
Tel: +44 (0) 1223 893295; Fax: +44 (0) 1223 894539
email: cisp@cisp-publishing.com; http://www.cisp-publishing.com

Advances in Electrometallurgy 2011 ***9*** *(4) 203–206*
Translated from Sovremennaya Elektrometallurgiya 2011 ***9*** *(4) 3–5*

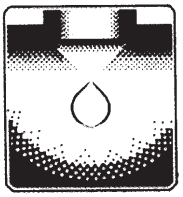

ELECTROSLAG TECHNOLOGY

Refining the crystal structure of hollow titanium ingots in magnetically controlled electroslag melting

I.V. Protokovilov

EO .P aton Electric Weld ng Institute,K iev

Investigations were carried out into the special features of the formation of the crystal structure of hollow ingots in electroslag melting under the effect of the external magnetic field. It is shown possible to define the structure of the billet as a result of the hydrodynamic effect on the liquid metal pool, generated by the external longitudinal magnetic field.

In Ref. 1–3 it was shown possible to refine the crystal structure and increase the physical and chemical homogeneity of billets of titanium alloys in the process of magnetically controlled electroslag melting (MCESM). These effects are achieved as a result of the hydrodynamic effect on the liquid metal pool, generated by the melting current and the external magnetic field.

The aim of the present work is the investigation of the possibility of refining, during MCESM, the crystal structure of hollow titanium billets used as blanks for the production of seamless cold- and hotrolled pipes. The coarse-grained structure of the blanks, typical of cast metal, greatly complicates or prevents further deformation. Therefore, the structural factor, together with the technical and economic parameters, is the most important characteristic which determines the efficiency of production of the hollow tubular blanks by the metallurgical methods.

Experimental melts were produced in a chamber electroslag furnace in argon (Fig.1). The consumable electrode, produced from six titanium bars with a diameter of 35mm (Fig. 2), was remelted in a solidification mould with a diameter of 160 mm under AN-T4 flux. The

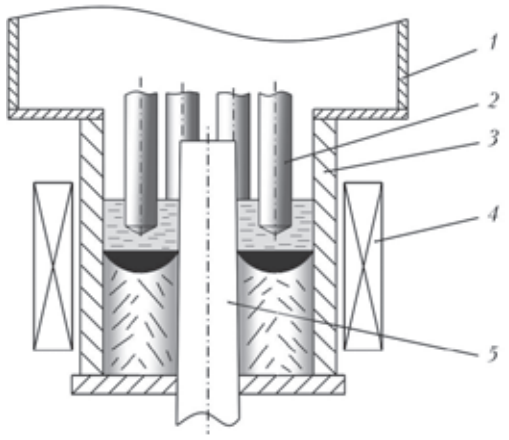

Fig. 1. Diagram of magnetically controlled electroslag melting of hollow billets: 1) the furnace chamber; 2) the consumable electrode; 3) external solidification mould; 4) electromagnetic system; 5) the internal solidification mould.

Fig. 2. External appearance of the consumable electrode

Table 1. The melting conditions of hollow billets

Hollow ingot diameter, mm		U, V		Parameters of electromagnetic effect		
Outer	Inner			B, T	t_p, s	t_b, s
160	40–50	36	4500	-	-	-
160	40–50	36	5000 (1200)	0.20–0.28	1	10

Comment. The values in the brackets are the minimum current during the pulse of the magnetic field; t_p is the duration of the pulse of the electromagnetic effect, t_b is the duration of the break between the pulses of the electromagnetic effect.

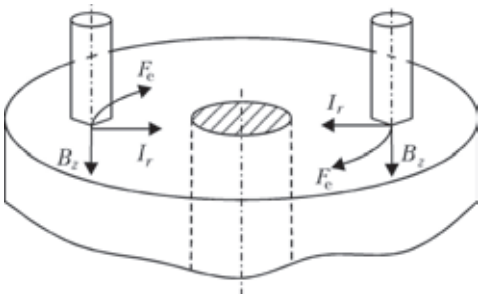

Fig. 3. Direction of the electromagnetic force in MCESM of hollow billets: B_z – the axial component of the induction of the external magnetic field; I_r – the radial component of the melting current; F_e – the electromagnetic force.

diameter of the internal conical solidification mould was 40–50 mm.

Melts were produced both without and with the electromagnetic effect of the axial (longitudinal) magnetic field, generated by a solenoid encircling the solidification mould. The electromagnetic effect was applied in individual pulses of a direct magnetic field, alternating with breaks. The melting conditions are presented in Table 1.

The mechanism of the hydrodynamic effect in melting of the hollow ingots consists of the interaction of the axial component of the external magnetic field B_z with the radial component of the melting current I_r in a metallurgical pool. As a result of this interaction, the azimuthal electromagnetic force $F_e = I_r \times B_z$, resulting in the rotation and vibration of the pool around the axis of symmetry (Fig. 3), forms in the current-carrying melt. The efficiency of the electromagnetic effect in melting of the hollow billets

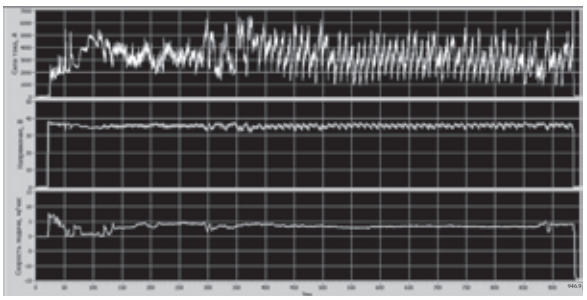

Fig. 4. Recording of the melting conditions in pulsed electromagnetic effects.

Fig. 5. A hollow billet of VT1 alloy.

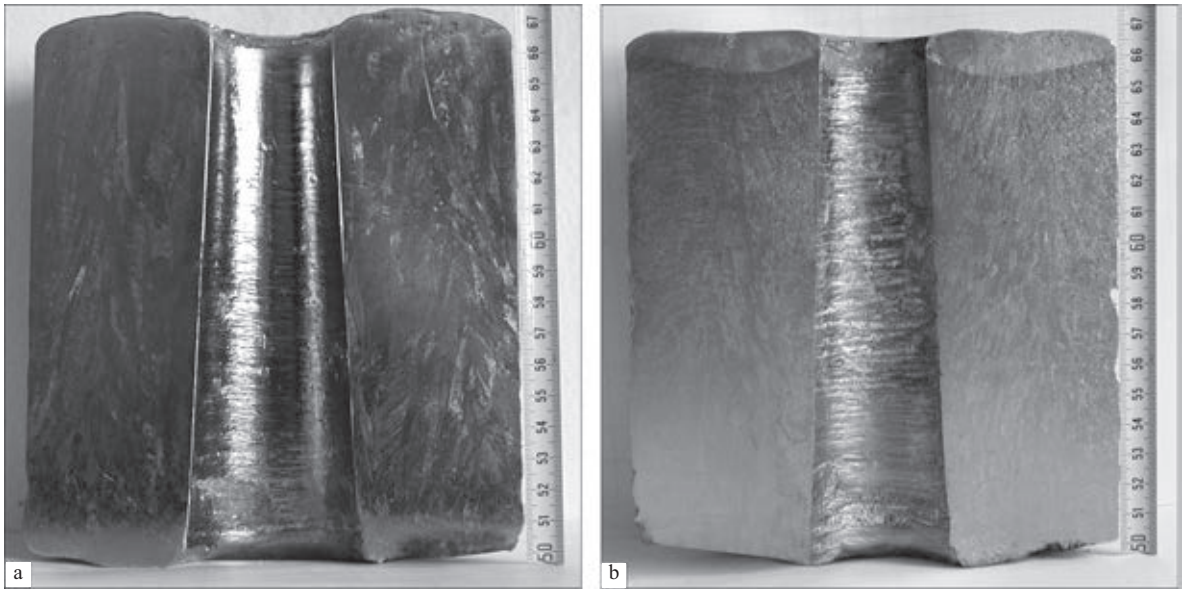

Figure 6. Macrostructure of the hollow titanium billets, produced without (a) and with the effect of the electromagnetic field (b).

increases as a result of the application of the internal current-conducting solidification mould and, consequently, the radial component of current in the metallurgical pool I_r and, correspondingly, the level of the electromagnetic force F_e increase.

The experiments with the pulsed effect of the longitudinal magnetic field in melting of the hollow ingots showed that, as in MCESM of solid ingots of titanium alloys [1], the presence of the regular phenomenon on when the pulsed effect of the magnetic field results in the periodic changes of the melting current (Figure 4). During the pulse of the magnetic field, the melting current decreases, and in the break period it is restored to the initial value. This reduction of current during the pulse of the magnetic field is caused mainly by the deformation of the free surface of the slag pool under the effect of the rotation of the slag and by the reduction of the depth of emotion of the consumable electrode in the slag. In this case, at a magnetic induction in the melting zone of up to 0.28 T, the process is of the quasi-stationary nature and does not lead to any large reduction of the stability of the electroslag remelting process and the quality of formation of the billets. No large defects are found on the external and internal surfaces of the billets (Figure 5).

The macrostructure of the billets, melted with and without the effect of the electromagnetic field, is shown in Fig. 6. In both cases, the structure of the metal is dense, without pores, slag inclusions and other defects. The billets, produced without the external effect, are characterised by the presence of large columnar crystals oriented mostly in the direction parallel to the axis of the billet (Fig. 6a). The longitudinal size of the crystals is 20–50 mm, the transverse size 3–7 mm.

Under the electromagnetic effect the structure of the metal is more homogeneous and fine-grained and consists of the crystals elongated in the direction of heat removal with the mean size of 2 × 10 mm and the equiaxed crystals, 2–4 mm in size (Fig. 6b).

The mechanism of refining of the structure is based on the fracturing effect on the growing crystals of the electromagnetic vibrations with a frequency of 50 Hz, produced by the interaction of the direct magnetic field with the alternating melting current, and also by the hydrodynamic ‘shocks’ taking place at the moment of activation and switching off

the magnetic field.

It should be mentioned that the pulsed effect of the magnetic field results in cyclic changes of the melting current and, correspondingly, portional heat generation in the slag pool. Consequently, the mechanisms of the thermal effect of solidification of the metal are added to the hydrodynamic mechanisms of refining the structure of the metal.

Thus, it has been shown possible to refine the crystal structure of the hollow titanium billets in MCESM by the pulsed electromagnetic effects on the melts of the slag and the metallic pools by the longitudinal magnetic field. The homogenising and refining of the structure of the metal of the tubular blanks increases the stability of the process of thermomechanical treatment of the blanks and the quality of the products.

References

1. Kompan, Ya.Yu., et al., Sovremennaya Elektrometallurgiya, 2007, No. 4, 3-7.
2. Protokovilov, I.V., Magnetically controlled electroslag melting of multicomponent titanium alloys, Dissertation, E.O. Paton Electric Welding Institute, Kiev, 2006.
3. Kompan, Yu.Yu. and Protokovilov, I.V., Technological aspects of magnetically controlled electroslag melting of titanium alloys, in: Proceedings of the International scientific and technical conference: Special electro-l metallurgy, yesterday, today and tomorrow, Kiev, 2002, 256-262.

Submitted 22.9.2011

Advances in Electrometallurgy 2011 ***9*** *(4) 207–210*
Translated from Sovremennaya Elektrometallurgiya 2011 ***9*** *(4) 6–8*

ELECTRON BEAM PROCESSES

Producing shape memory titanium alloys by electron beam melting with a cold hearth

V. Berezos and N.P. Trigub

EO .P aton Electric Weld ng Institute,K iev

The results of experimental studies of the production of an alloy based on titanium TiNi by electron beam melting are presented.

Shape memory alloys have been used widely in the last couple of decades because they make it possible to realise the service characteristics of structures and devices which cannot be obtained using other materials. They are characterised by a wide range of applications depending on the martensitic transformation temperature and mechanical properties. They are used in nuclear power engineering, engineering, aerospace and household technology, instrument making, special machine construction, etc [1–6]. As shown by the experience accumulated throughout the world, medical devices represent a highly promising area of application of these alloys [7].

At present, more than 10 shape memory effect alloys based on different elements are available: TiNi, TiNb, PtTi, and others [8]. However, the best-known and important alloy is the TiNi alloy (Nitinol) with a distinctive shape memory effect the temperature range of which can be controlled with high accuracy by adding various admixtures to the alloy. The application of Nitinol is determined by the fact that it has a rare combination, for alloys of this type, of the high structural, technological and functional properties of the shape memory effect and superplasticity. These alloys are characterised by high elastic properties, are capable of changing the shape during temperature changes and do not fracture in the conditions of alternating loading. The alloy is characterised by high shape memory characteristics, high-strength with a low elasticity modulus in comparison with stainless steel, and is also characterised by the high level of the damping capacity of the material and corrosion resistance.

The experimental results show that these alloys are not toxic, have no cancerogenic effect on the surrounding tissue, have high parameters of corrosion resistance in the living organism tissue and biological compatibility and, consequently, are used in medicine as long-term functioning materials implanted in

the organism [7].

However, the application of any structural material depends not only on its physical-mechanical characteristics but also on other characteristics, such as technological properties, availability and cost. The complicated nature of metallurgical production of the TiNi alloy is another delaying factor for extensive application. To produce semifinished products with the guaranteed triggering temperature, it is necessary to use expensive equipment. Consequently, the cost of components is high.

In most cases, TiNi alloys are produced by a multistage technological process [8]. In the presence of titanium in the alloy which easily bonds nitrogen and oxygen, the essential condition for production is the application of vacuum equipment or shielding atmosphere (helium or argon).

To produce high-quality alloys with high mechanical properties, it is necessary to select correctly the primary components. In most cases, the charge consists of iodised titanium or titanium sponge, compacted into briquettes, and also N-0 or N-1 nickel.

To produce the uniform chemical composition and the cross-section and the length of the ingot, it is necessary to apply double or triple remelting. The TiNi alloys are melted using vacuum-induction and arc methods [8]. The initial ingot is produced in graphite furnaces by vacuum induction melting. Consequently, an efficiently mixed alloy can be produced. To improve the chemical composition, structure and homogeneity, this is followed by remelting in a vacuum arc furnace with a consumable electrode.

The shape of effect materials with a higher titanium content belong to chemically 'aggressive' melts. They are characterised by high wetting capacity and complete spreading of the melt on the surface of standard refractory materials (oxides, carbides, nitrides, graphite, etc). The melt can penetrate into cracks and pores made of a refractory material, cause decay and failure of the material and, consequently, saturation and contamination of the alloy with the products of interaction with the elements of the crucible material, in particular oxides, nitrites, titanium carbide. This is caused by the high affinity of this metal for oxygen, nitrogen and carbon [8].

The impurities, penetrating into the alloy as a result of interaction with the crucible, have a strong effect on the quality of the TiNi alloy. Even small changes in the proportions of the components leads to the variation of the martensitic transformation temperature. These contaminated alloys not only change the martensitic transformation temperature but may also lose capacity for the transformation [9].

Thus, the production of the high-quality TiNi alloys not reduced to simple melting of the metals and maybe classified as belonging to the group of 'high' technology processes.

The production of semifinished products based on TiNi alloys with the required chemical composition and the level of the mechanical properties has been mastered only in several countries [10].

The E.O. Paton Electric Welding Institute, Kiev, has accumulated a large amount of experience in the area of melting billets of titanium intermetallics by the method of electron beam melting with a cold hearth [11].

Electron beam melting with a cold hearth is characterised by a high level of refining capacity. The formation of the guaranteed chemical composition in a narrow concentration range with the required chemical homogeneity in the billets in melting of the alloys is the result of application of the cold hearth.

The aim of the present work is to carry out experiments and develop technology for producing billets of Ti-46% Ni-54% alloy in electron beam melting with an intermediate container.

Experimental melts of the billets with a diameter of 165 mm of the TiNi alloy were produced in UE-208M equipment (Fig. 1).

Equipment can be used to melt cylindrical billets with a diameter of up to 300 mm and up to 2000 mm long, and also rectangular ingots with a size of 450 × 145 mm, up to 1500 mm long.

The charge materials were in the form of sheets of VT1-0 titanium alloy and sheets

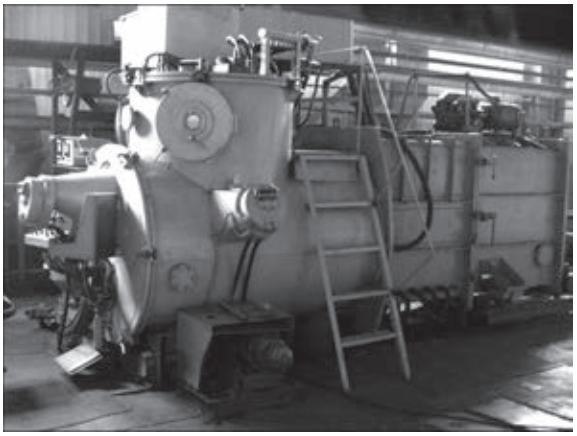

Fig 1. UE-208M electron beam equipment.

Fig 2. The process of melting TiNi alloy

of cathodic nickel N-1. Since titanium and nickel are characterised by similar values of the melting point (1645 and 1455°C, respectively), and also the reputation at the melting point, experiments were carried out using the method in which the charge in the required percentage proportion was placed in a consumable titanium box. After loading the charge, equipment was evacuated. Initially, the charge was melted in a cold hearth and the liquid metal was periodically discharge into the copper watercooled solidification mould to produce a billet of the required length (Fig. 2).

At the end of melting the shrinkage cavity was displaced, the ingot was cooled in the conditions of vacuum to complete solidification.

Figure 3 shows a billet of TiNi alloy.

Fig 3. A billet of TiNi alloy.

To find internal defects in the form of non-metallic inclusions, pores and various discontinuities in the produce billets, the latter was inspected by ultrasound inspection using the echo-pulsed method with contact control using UD4-76 equipment (Fig. 4).

No pores, discontinuities or shrinkage-type defects were found in the billet.

The composition of the TiNi alloy was investigated by chemical analysis. Samples were taken along the billets at a depths of 5 mm from the surface and in the radial direction (across the billets) at radii of 70, 50 and 30 mm. Three zones – upper, lower and the centre of the billet – were investigated. The results of chemical analysis of the TiNi alloy show that the deviation of the content of the elements in the billets both along the length and in the cross-section does not exceed 0.2% and this is regarded as a satisfactory result [12].

Thus, the proposed technology and experimental melts of the TiNi alloy, produced by electron beam melting with a cold hearth, showed the high efficiency of using the cold hearth for producing high-quality TiNi ingots for purposes of the industry and medicine. As

Fig 4. UDF4-76 ultrasonic defectoscope.

a result of the development of this technology Ukraine belongs in the small group of countries capable of producing these alloys.

References

1. Zelenov, B.A.,et al., Alloys with cotrolled functional properties–prototype of intellectual materials, in: Materials with the shape memory effect, proceedings, part 3, St Peterburg, 1995. 55–58.
2. Ionaitis, R.R., et al., ibid, part 2, 133–134.
3. Ryklina, E.P. et al., ibid, part 2, 51–54.
4. Likhachev, V.A., et al., ibid, part 3, 59–61.
5. Voronkov, A.V. and Likhachev, V.A., ibid, part 1, 83.
6. Kravchenko, Yu.D., et al., ibid, part 1, 58–61.
7. Gyunter, V.E., et al., Titanium nickelide. Medical material of a new generation, MITs, Tomsk, 2006.
8. Krasovs'kii, P., Adgeziya Raspl. Paika Mater., 2009, No. 42, 95–102.
9. Anokhin, S.V., et al., in: Shape memory material, Proc., part 1, St Peterburg, 1995, 29–33.
10. Kanyukov, V.N., et al., Development of scientific and technical solutions in medicine, textbook, Orenburg State University, Orenburg, 2008.
11. Zhuk, G.V., et al., Sovremennaya Elektrometallurgiya, 2003, No. 20–22.
12. Aleksandrov, A.V., et al., Titan, 2010, No. 2, 36–41.

Submitted 20.4.2011

Advances in Electrometallurgy 2011 ***9*** *(4) 211–214*
Translated from Sovremennaya Elektrometallurgiya 2011 ***9*** *(4) 9–12*

Optimisation of the technology of electron beam melting of molybdenum by mathematical modelling

V.O. Mushegyan

Paton Armeniya Scientific and Technical Centre, E.O. Paton Electric Welding Institute, Kiev

Series of numerical experiments have been made for determination of optimum conditions of melting the molybdenumingots into a water-cooled mould. The effect of technological parameters of melting (power and distribution of electronbeam heating of metal in mould, frequency and temperature of charge overheating) on characteristics of ingot solidificationwas analyzed. The degree of effect of each of parameters in technologically allowable intervals was established.

The method of heating of metal used in electron beam melting makes it possible to redistribute the density of the heat flow in a wide range of the values irrespective of the productivity of melting of the metal with sufficiently high flexibility as a result of focusing the electron beam scanning the heated surface with the beam. Consequently, it is possible to influence purposefully the thermal state of the liquid pool in the solidification mould for the formation of the flat solidification front [1].

To utilise these possibilities, a uniform heat flow with local concentration in the vicinity of the solidification wall is produced in the central zone of the surface of the metal pool [2]. Central heating compensates the heat losses by the metal as a result of evaporation and radiation on the free surface, and peripheral heating compensates the heat removal into the wall of the watercooled solidification mould.

To determine the optimum parameters of melting of molybdenum in electron beam equipment with a cold hearth, corresponding to the minimum depth of the liquid pool and the flat solidification front, investigations were carried out using the model of electron beam melting of molybdenum in a continuous watercooled solidification mould [3]. The process of melting of a solidification mould with a diameter of 70 and 100 mm was simulated. During the process, the liquid metal was periodically supplied from the cold hearth into the solidification mould with time breaks between pouring the individual portions. The basic regime in the calculations was the electron beam melting regime applied in the experiments [3] (Table 1).

The main parameters of distribution of the electron beam heat flow are: D_R – section along the radius of the surface of the pool with 90% of the power of the peripheral heating W_2, distributed in accordance with

Table 1. Technological parameters of the basic (1) and calculated (2) conditions at the billet diameter of D = 7 cm, the depth of the pool l_z (r = R) = 0.2 cm

Condition No.	W_1	W_2	W_t	l_z (r = 0)
	kW			
1	8.4	49.2	60.0	0.60
2	7.4	51.2	56.6	0.38

Comment. Here W_t is the total power

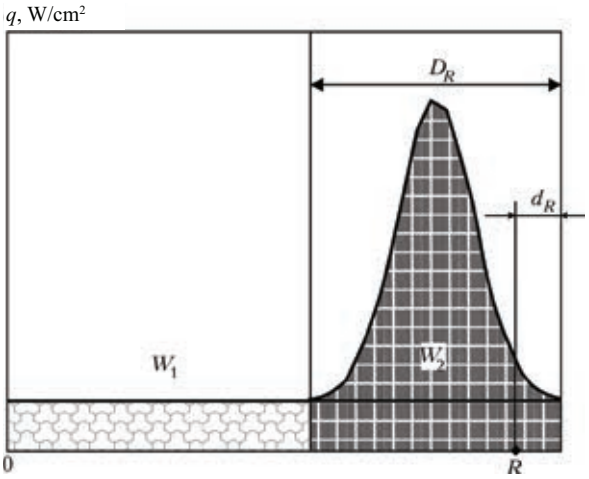

Fig. 1. Diagram of the distribution of the power of heating the metal q on the surface of the pool in the solidification mould.

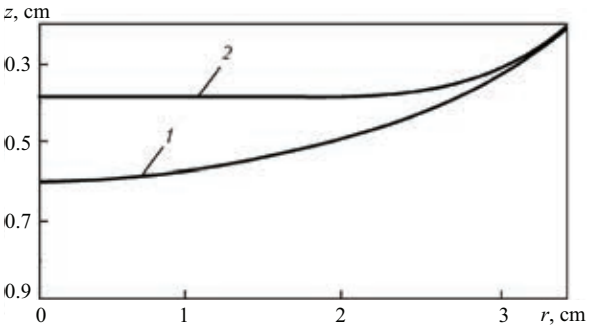

Fig. 2. Geometry of the liquid pool at the moment of completion of the break between the pouring cycles (D = 7 cm): z is the distance to the surface of the pool.

the Gauss law; d_R – displacement of DR to the solidification mould; W_1 – the power of central heating, uniformly distributed in the section 0…(D_R–d_R) of the surface of the pool (Fig. 1).

Figure 2 shows the geometry of the liquid pool at the moment of completion of a break between the individual pouring cycles for the two variants of heating the pool surface (Table 1): basic (1) and the one produced with the variation of the parameters W_1, W_2 (2).

The curves in Fig. 2 shows that by varying W_1, W_2, it is possible to produce a flatter solidification front in comparison with the basic variant, with a lower thermal power of heating (Table 1). This result can be achieved by reducing the density of heating in the central part of the pool and by increasing the density

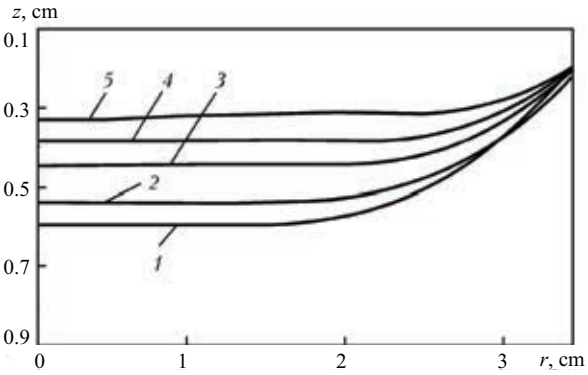

Fig. 3. Geometry of the pool at the moment of completion of the break between the pouring cycles at different values of dR: 1) 0; 2) 0.2; 3) 0.4; 4) 0.6; 5) 0.9 cm.

Table 2. Optimised heating conditions of the Mo billet in a solidification mould with a diameter of 70 and 100 mm

D	d	W_t	W_1	W_2
cm			kW	
7	0.6	50.808	6.562	44.245
10	0.4	77.694	17.273	60.420

in the vicinity of the solidification mould wall (Fig. 3). The zone of maximum temperature superheating of the surface of the tool is displaced from the axial to peripheral part of the pool, and according to the calculations, the superheating of the metal above the melting point increases by 60°C. For an ingot with a diameter of 100 mm, the qualitative pattern recorded in the experiments was the same.

A series of numerical experiments was carried out with the variation of displacement d_R of the electron beam to the wall of the solidification mould. Figure 3 shows the results of calculations for a billet with a diameter of 7 cm for different values of d_R.

As indicated by the figure, the increase of d_R produces a flatter solidification front but, as shown by the calculations, the larger displacement of the region of peripheral heating to the wall of the solidification mould results in the need to increase the heat input W_t by a factor of 1.5. Taking the special features into account, subsequent optimisation calculations were carried out using the parameters d_R according to Table 2, which produce the relatively flat solidification front with the moderate increase of the thermal power of

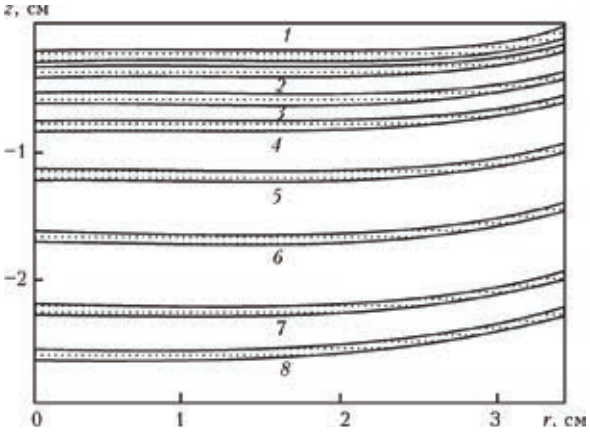

Fig 4. Range $T_X - T_L$ at different values of the power W_t of heating the pool surface, kW: 1) 54.4; 2) 56.8; 3) 59.6; 4) 62.4; 5) 67.4; 6) 7.3; 7) 70.2; 8) 83.8 kW); D = 7 cm.

Table 3. Technological thermophysical characteristics of different melting conditions (solidification mould D = 7 cm)

$l_z(r=R)$, cm	W_t	W_1	W_2 (kW)	G, °C/cm	dt, s	$l_z(r=0)$, cm
0.1	55.387	7.374	48.012	230.48	2.314	0.28
0.2	56.860	7.475	49.386	229.01	2.329	0.40
0.4	59.620	7.642	51.979	227.37	2.350	0.61
0.6	62.414	7.780	54.634	226.92	2.346	0.82
1.0	67.385	7.723	59.661	222.70	2.390	1.22
1.5	72.974	7.020	65.953	221.90	2.400	1.71
2.0	78.215	6.867	73.347	220.10	2.450	2.28
2.3	83.805	6.165	79.639	217.00	2.500	2.64

heating the pool surface.

To evaluate the effect of the total heating power of the pool surface W_t on the solidification parameters of the liquid metal, the range of the values l_z ($r = R$) was selected in accordance with Table 2. The values of W_1, W_2 were selected to ensure that the front was flat without deflection.

Figure 4 shows the geometry of the pool and the region with the established superheating of the metal ($T_X - T_L$, where T_X = 2637, T_L = 2670°C – the temperature of the superheated metal and the melting point, respectively). Table 3 and gives the results of the calculations indicating that it is not rational to increase the intensity of heating the pool surface because the increase of the heat input does not increase the solidification parameters of the liquid metal. On the other hand, with a reduction of the power of heating the liquid metal in the solidification mould the thermophysical characteristics of the solidification process of the molybdenum improved; the temperature gradient G along the direction of movement of the solidification front increases and the time period of cooling dt decreases (the cooling rate increases correspondingly). Similar relationships were obtained for 100 mm diameter billets.

Investigations were carried out into the effect of periodicity of pouring and superheating of the metal supplied into the solidification mould above the melting point on the thermal

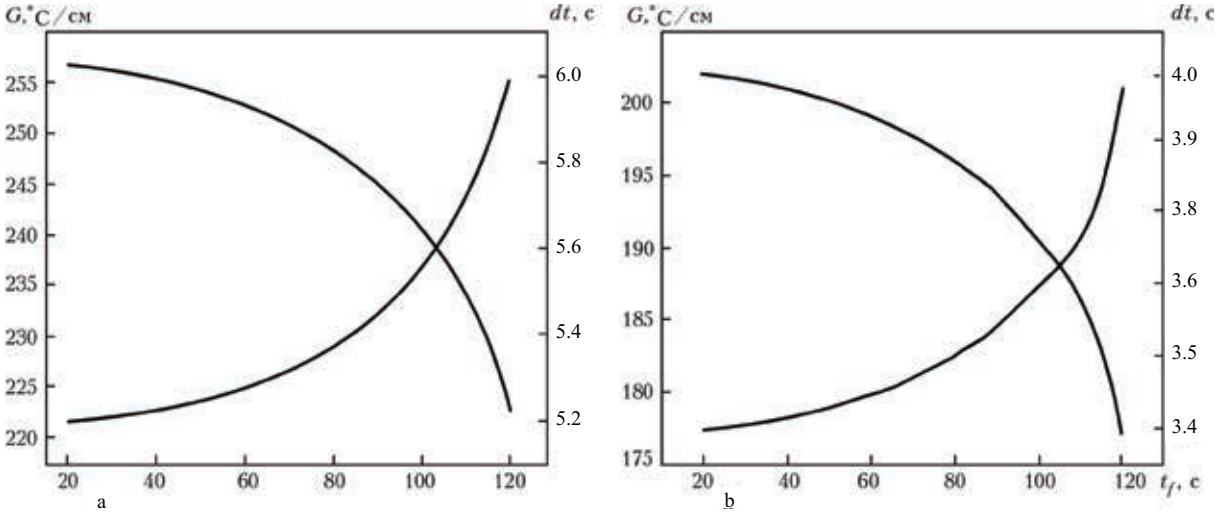

Fig. 5. Dependence of the temperature gradient ahead of the solidification front and the holding time of the metal tf in the given temperature range (2637–2670°C) on casting time (the period of supply of metal 120 s) at D: a) 7; b) 10 cm.

Table 4. Dependence of the solidification parameters on the superheating temperature ΔT

ΔT	$l_z\,(r=0)$	$l_z\,(r=0)$	t, s	G, °C/cm
		$D = 7$ cm		
0	0.76	0.20	5.19	256.70
40	0.76	0.20	5.19	257.02
80	0.76	0.20	5.19	256.97
140	0.76	0.20	5.19	256.85
		$D = 10$ cm		
0	0.370	0.099	3.389	202.36
40	0.371	0.099	3.389	202.33
80	0.373	0.099	3.391	202.22
140	0.375	0.099	3.393	202.07

state of the billets. Pouring of metal with a period of 120 s was simulated. In this procedure, the pouring time was varied in the range 20–120 s, and the break between the pouring cycles was 0–100 s.

Figure 5 shows the mean values for the period showing the effect of the ratio of the pouring time and the break time on the parameters of solidification of the liquid pool. The experimental data show that at a ratio of the pouring time and the break time of 20:100 and 120:0 (continuous pouring) the holding time in the given solidification temperature range and the temperature gradient in front of the solidification front changed by 13%, with the best parameters obtained at a minimum pouring time of 20 s.

The calculation results also show (Table 4) that the variation ΔT (superheating of the metal, supplied into the solidification mould, about the liquidus temperature) in the range 0–140°C does not result in any significant variation of the parameters of the liquid metal pool. Consequently, the increase of the degree of superheating of the poured in metal is not recommended because this increases the energy losses in the stage of the cold hearth.

Conclusions

1. The calculation results show that the application of central and peripheral heating of the metal in the solidification mould in melting molybdenum ingots with a diameter of 7 and 10 cm in the electron beam furnace makes it possible to produce the almost completely flat solidification front, with the minimum depth of the liquid pool.

2. The main parameters, influencing the process of solidification of molybdenum in electron beam melting in a cold hearth – the power of electron beam heating, displacement of the beam to the solidification mould, the ratio of the pouring and break time, were determined. At the same time, superheating of the portions above the liquidus temperature does not have such a strong effect.

References

1. Paton, B.E., Electron beam melting, NaukovaDumka, Kiev, 1997.
2. Zhuk, G.V., Sovremennaya Elektrometallurgiya, 2008, No. 2, 17–20.
3. Mushegyan, V.O. Sovremennaya Elektrometallurgiya, 2011, No. 3, 13–16.

Submitted 26.10.2011

Advances in Electrometallurgy 2011 ***9*** *(4) 215–217*
Translated from Sovremennaya Elektrometallurgiya 2011 ***9*** *(4) 12–13*

Purification of silicon to remove phonon and doping impurities in electron beam crucibleless zone melting

E.A. Asnis, N.V. Piskun and I.I. Statkevich

EO .P aton Electric Weld ng Institute,K iev

The data are presented on the effect of the sterility of the vacuum melting chamber on the content of the phonon and doping impurities in single crystal silicon produced by electron beam crucibleless zone melting.

The problem of purification of silicon to remove the impurities, especially oxygen, is very important when using silicon as a radiation-resistant material, in particular, for producing highly efficient counters of nuclear radiation, solar batteries, devices situated on the external surface of stations and subjected to the hard radiation with high-energy particles. The presence of oxygen in silicon reduces the operating speed of electronic devices and is the reason for non-reproducibility of the parameters of various devices, such as pulsed and switching diodes, microwave diodes, etc [1].

In some cases, in the production of single crystal silicon with *p*-conductivity, it is necessary to purify silicon also to remove doping impurities, for example phosphorus.

At present, the purity of silicon with respect to the doping impurities has been improved to $1\cdot10^{13}$…$1\cdot10^{14}$ at/cm^3, and the content of the phonon impurity – oxygen in the crystals grown by different methods to $1\cdot10^{17}$…$1\cdot10^{18}$ at/cm^3.

The process of electron beam crucibleless zone melting is accompanied by the purification of silicon to remove doping phonon impurities [2], as a result of sublimation, caused by the zone recrystallisation is also desorption of the impurities from the surface of the specimen at temperatures close to solidification temperature. Using this method, impurities with the vapour tension higher than that of silicon are removed from the melt [3].

The impurity content of silicon is influenced by the residual atmosphere of the melting vacuum chamber in which zone electron beam melting is carried out, and the degree of vacuum in the chamber is one of the main parameters. To determine the possibility of purification of silicon to remove oxygen, calculations were carried out to determine the oxygen concentration in the residual atmosphere of the vacuum chamber:

$$P = \mathrm{nkt}, \qquad (1)$$

where P is the partial pressure of oxygen, Pa; n is the number of oxygen atoms, cm^3; k is the Boltzmann constant equal to $1.38\cdot10^{-23}$ J/deg; T is the temperature in the chamber, K. The residual pressure in the chamber, prepared for melting silicon, is usually $2\cdot10^{-5}$ torr ($2.7\cdot10^{-3}$ Pa) at a temperature of 300 K. It may be assumed that the ratio of the partial pressure of oxygen to the residual pressure in the chamber, as in the air atmosphere, is equal to 1:5. Consequently, the partial pressure of oxygen taking into account this ratio is 5.7 ·

10^{-4} Pa. Equation (1) was used to calculate the oxygen concentration in the vacuum as $n = 2.8 \cdot 10^{11}$ at/cm^3. This should support the desorption of impurities from the surface of the silicon specimen during melting.

When the chamber is opened, air penetrates into it and high-intensity adsorption of the gas molecules and moisture takes place on the surface of equipment and the chamber wall. This reduces the vacuum in the chamber. The methods of preparation of the vacuum chamber to increase the vacuum in the chamber, such as preheating of the chamber to 400-450°C, infrared and ultraviolet irradiation of the chamber walls, fittings, etc. However, they are not completely suitable because of a number of reasons.

The melting vacuum chamber include various rubber interlayers, gaskets, fluoroplastic components, etc and this greatly complicates the application of the thermal method of purification. The irradiation of the chamber walls with infrared and ultraviolet beams complicates the technological process of preparation of the chamber.

An effective and simple method of preparation of the vacuum chamber to increase the vacuum is the flushing with high purity helium during pumping.

In flushing the chamber with helium, the latter actively removes the adsorbed impurities, acting as a unique 'broom' [4]. The helium molecules, impacting on the walls of the chamber and the fittings, weaken the force of interaction of the adsorbed molecules and gases and moisture, and create suitable conditions for desorption and removal during pumping, i.e., intensify the degassing of the chamber.

This process should be carried out to reduce the possibility of contamination of helium with active gases, especially oxygen, as a result of its disruption in heating the chamber, and also equipment in melting.

The experimental results show that to purify the single crystal silicon in electron beam crucibleless zone melting, especially to remove oxygen, it is necessary to ensure that in leakage into the melting chamber (arrival of active gases through micro-irregularities in the vacuum seals and desorption from the walls of the chamber and the fittings) does not exceed $2 \cdot 10^{-4}$ l·torr/s.

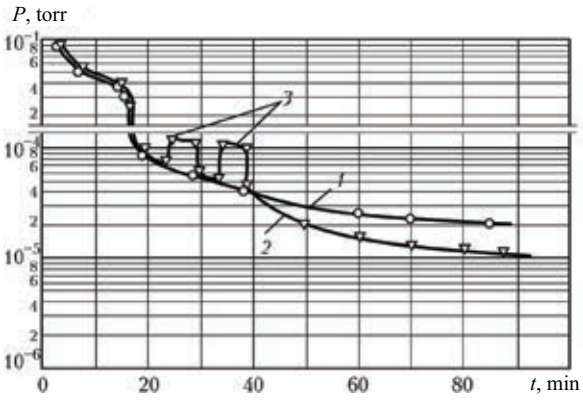

Fig. 1. Effect of flushing with He on the vacuum in the chamber for different pumping times: 1) pumping with flushing with He; 2) the same, with flushing; 3) flushing.

The chamber was flushed with He through a special inlet valve at a helium flow rate of 30 cm^3/min. Two 10 min flushing cycles were applied. The period between the flushing cycles was 10 min. The number of flushing cycles and the break between the cycles were determined in relation to the duration of minimum pumping of the chamber to ensure the working regime ($2 \cdot 10^{-5}$ torr).

Figure 1 shows the effect of flushing with helium on the vacuum in the chamber for different pumping times. As indicated by the graph, after flushing, the vacuum is approximately doubled (from $2.1 \cdot 10^{-5}$ to $1.2 \cdot 10^{-5}$ torr) for the same pumping time. The inleakage was $2 \cdot 10^{-4}$ l·torr/s and the volume of the melting chamber of 0.028 m^3.

Investigations by infrared spectroscopy show that after flushing the chamber with He, and with increase of the vacuum, the oxygen content decreases by more than an order of magnitude (from $6 \cdot 10^{16}$ to $5 \cdot 10^{15}$ at/cm^{-3}) in comparison with the vacuum, produced in the chamber without reducing (Fig. 1).

The effect of preparation of the vacuum melting chamber on the phosphorus content in silicon was investigated. The results of

Hall measurements and electron paramagnetic resonance show that when using the chamber preparation methods, described previously, the phosphorus content decreases by an order of magnitude (from $8 \cdot 10^{13}$ to $1 \cdot 10^{13}$ at/cm^3).

Thus, the improvement of the sterility of the melting vacuum chamber in electron beam melting of silicon greatly reduces the content of alloying and doping impurities in the produced single crystals.

References

1. Paton, B.E., et al., Kosmichna nauka i tekhnologiya, 2003, vol. 9, No. 5/6, 30–32.
2. Pfann, B., Zone melting, Mir, Moscow, 1977.
3. Nepomnyashchikh, et al., Materialy elektronnoi tekhniki, 2002, No. 4, 16–24.
4. Stoner, D.R. and Lessman, G.G., Welding Journal, 1965, vol. 44, No. 8, 337–346.

Submitted 23.3.2011

Advances in Electrometallurgy 2011 ***9*** *(4) 218–224*
Translated from Sovremennaya Elektrometallurgiya 2011 ***9*** *(4) 14–19*

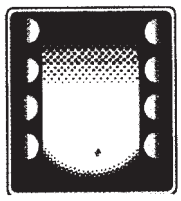

VACUUM INDUCTION MELTING

Cooled solidification moulds for the formation of ingots with the electromagnetic effect on the melt

I.V. Sheiko, V.A. Shapovalov, V.V. Yakusha, Yu.A. Nikitenko and D.M. Zhirov

E.O. Paton Electric Welding Institute, Kiev

Peculiarities of induction melting in a sectional mould and transfer of energy of the high-frequency electromagnetic field from the inductor to the metal pool are considered. It is shown that the sectional moulds represent units of complicated design, the functional capabilities of which are much wider than in moulds of a traditional design. They effect not only the ingot formation, but also on the transfer of electromagnetic field energy from the inductor or other electromagnetic system to the melt, thus increasing in some cases the technical-economical characteristics of remelting processes (for example EBR and ESR) and quality characteristics of the produced metal. The degree of energy transfer into the metal pool depends to a large extent on the design of water-cooled sections.

In the currently available remelting methods, based on the application of electric heat sources (vacuum-arc – VAR, electroslag – ESR, electron beam – EBR, and plasma-arc remelting PAR), the formation of the billets during melting takes place in a copper cooled solidification mould. The design solutions of these devices greatly differ and are determined in particular by the special features of the individual processes.

For example, the majority of the solidification moulds for VAR and ESR have the form of a watercooled ingot mould in which the shaping sleeve is produced from copper and placed into a steel shell (jacket). Cooling water is supplied into the ring-shaped gap between the sleeve and the shell. The height (length) of these solidification moulds is usually greater than the length of the billets because the billet is melted by remelting the consumable electrode directly in the solidification mould [1–3].

Formation of the billets in the EBR and PAR furnaces takes place as a result of the remelting of consumable billets which are placed above the solidification mould, and the billet during melting is extracted from the solidification mould. The height of such a solidification mould usually does not exceed the diameter of the melted billets because during melting a metallic pool forms in the solidification mould, and the billet is situated below the solidification mould [2, 4–7].

In the second half of the 20th century special attention was paid about and in this country to the methods of induction melt-

ing of high-reactivity metals in which the crucible made of a refractory material is replaced by the so-called cold crucibles or cooled sectional solidification mould. These processes are referred to as induction melting in a cold crucible (IMCC) and induction remelting in a sectional solidification mould (IRSSM) [8–15].

The source of thermal energy in IRSSM is the electromagnetic field generated by the alternating current flowing in the induction coil. The condition of energy transfer of the electromagnetic field in IRSSM differ from those in the conventional induction melting method because the wall of the sectional solidification mould is placed between the induction coil and the load.

In contrast to other remelting processes (VAR, ESR, EBR and PAR), in which the formation of the billets also takes place in the cooled solidification mould which is only the design element shaping the billet, in IRSSM the solidification mould is also used as an electrical engineering link in the electrical power circuit. Thus, the design of the sectional solidification mould control not only the quality of the melted billets but also the electrical engineering parameters of the process.

In the internal volume of the solidification mould as a result of the formation of induced current in the sections, the electromagnetic field is produced there. In addition to this, the electromagnetic field, generated by the current of the induction coil, penetrates through the gap between the sections. In the zone, situated opposite the joints in the sections, the strength of the electromagnetic field is considerably higher than in the zones opposite the sections.

The experimental results show that the path of current, induced in the sections, depends on the design of the sections. In the cross-section, each section has four walls with their functional purpose.

For example, in the outer wall, facing the induction coil, the current, generated by the electromagnetic field of the induction coil, is induced. The current passing in the internal wall of the section (facing the load) induces the occurrence in the surface layer of the load and, therefore, the internal wall of the section is used as an induction coil for the load. The radial walls of the sections are current suppliers ensuring the supply of current to the internal walls of the sections. Thus, to reduce the electrical losses in the solidification mould, it is necessary to reduce the length of the radial (lateral) walls of the sections.

For the same wall thickness of the sections, which is characteristic of the sections produced from the profiled copper pipe (Fig. 1a), the induced circular current flows uniformly through the wall thickness. If the wall thickness of the section is not constant, which is the case when using drilled channels for the flow of cooling water (Fig. 1b), the circular current passes along the shortest path. As a result, they bend edges at the contact of the radial and internal walls leading to the formation of the edge ‘dead’ zones on both sides of the internal wall. This reduces the length of the inducing part of the internal wall of the section, special in opera-

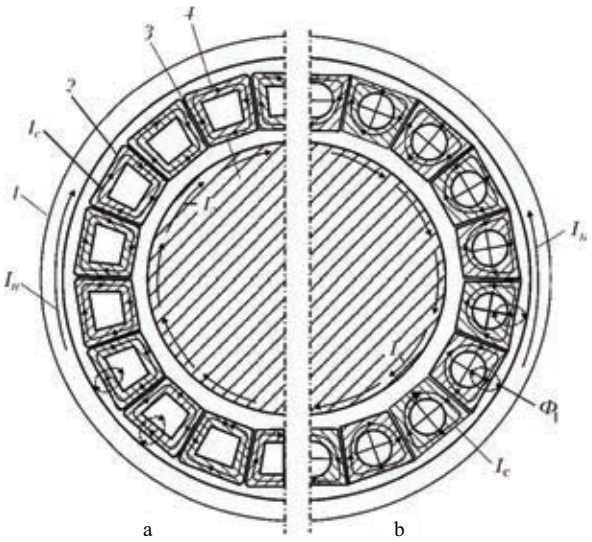

Fig. 1. Passage of current in the elements of the induction coil-solidification mould-load system in relation to the wall thickness of the section of the solidification mould: a) with the same perimeter; b) with different perimeter; 1) induction coil; 2) the sections of the solidification mould; 3) dielectric interlayer; 4) the load; II – the current used in the surface layer of the load; I_c – the current induced in the section; I_i – the current of the induction coil; Φ_1 – the magnetic flux of the section.

tion with the currents of the medium and low (2.5–8.0 kHz and less) because the reduction of the frequency of electrical current reduces the intensity of the surface defects and also the extent of regeneration in the load rapidly decreases. Consequently, the electrical efficiency of the induction coil–solidification mould–load system decreases.

The experimental results also show that in the prototype of the load, placed in a sectional solidification mould, whose sections are produced from profiled copper pipes, at a frequency working current of 2.5 kHz 36–40% of thermal energy is generated on average. In the same prototype of the load, placed in the solidification mould with the sections containing drilled channels for the flow of cooling water, only 27–32% of thermal energy is generated, i.e., 8–12% less.

According to the principle of formation of the billets, the sectional solidification mould can be divided into two groups: solidification mould–ingot moulds in which the billet is produced without displacement during melting in relation to the wall of the solidification mould; the solidification moulds in which the billets is extracted during melting using a special mechanism (sliding solidification mould).

Each of these methods is used widely in practice and has both advantages and disadvantages. The main advantage of melting the billets in the solidification mould–ingot moulds is the absence of displacement of the billet in relation to the wall of the solidification mould during melting. In this case, the solidification mould and the billets are not subjected to mechanical loading, caused by friction of the billet on the shaping wall of the solidification mould. This greatly increases the service life of the solidification mould. In addition to this, formation of the cracks in the billet produced from metals and alloys with low plasticity even at high temperatures is prevented.

A shortcoming of this method is the large metal requirement of the sectional solidification mould, complicated manufacturing technology and, correspondingly, high cost.

The advantages of the method with the withdrawal of the billets include the small metal requirement and the cost of sectional solidification mould because the total height of the shaping sleeve is usually not greater than two diameters of the billets. The main shortcoming of the method is that it cannot be used to melt billets from metals and alloys with low plasticity and, therefore, the process of withdrawal may be accompanied by the formation of transverse cracks resulting sometimes in fracture of the billets.

The solidification moulds for induction melting of the billets by withdrawal are structures consisting of a copper sectional sleeve and a water collector (Fig. 2, 3). The main technical characteristics of the solidification moulds are presented in Table 1.

The shaping sectional sleeve is produced from thick wall copper pipe (wall thickness 25 mm and greater) by milling radial grooves forming the longitudinal sections. To ensure

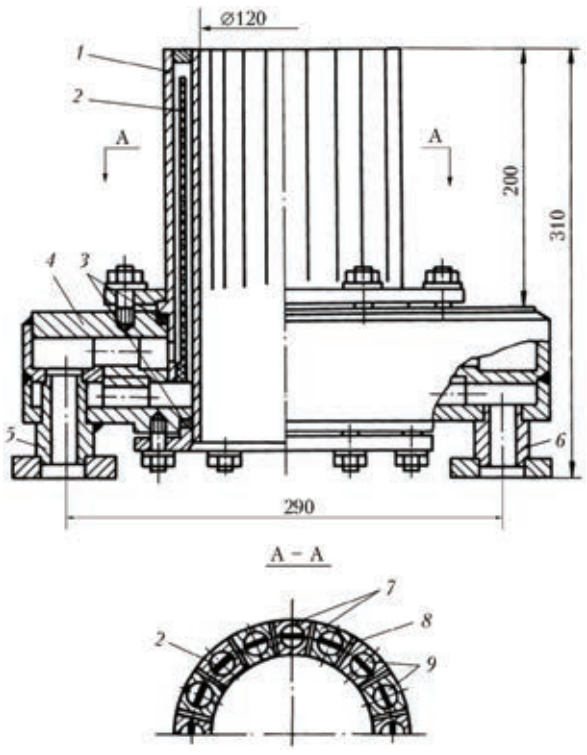

Fig 2. The design of the sectional (sliding) solidification mould for induction melting of billets with withdrawal during melting; 1) the shaping sleeve; 2) the deflector; 3) the sealing rings; 4) the water collector; 5) the nozzle for the supply of cooling water; 6) the nozzle for the removal of water; 7) sections; 8) dielectric interlayer; 9) the channels for the waterfall.

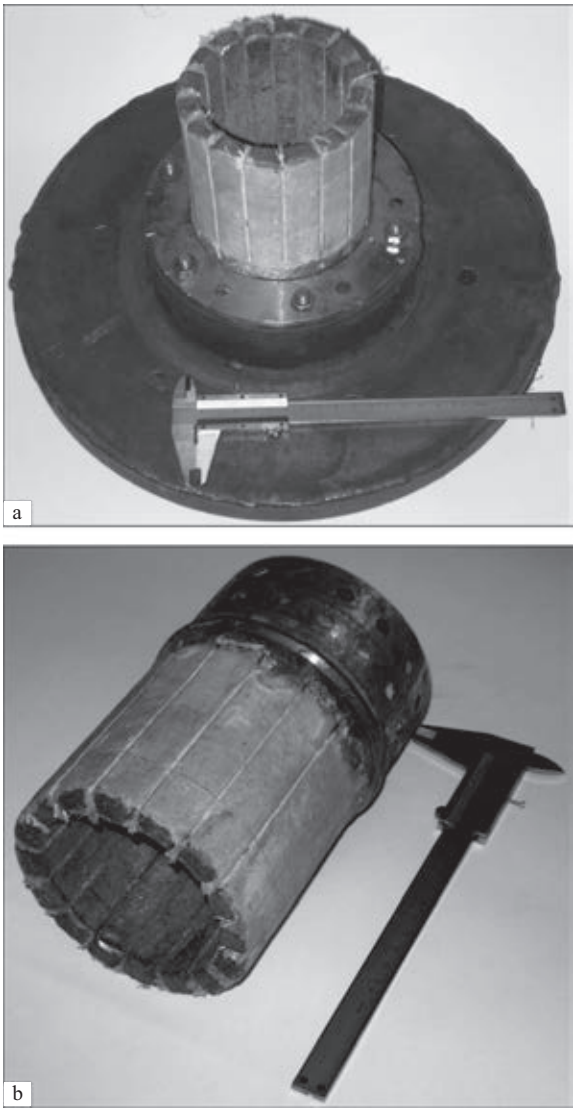

Fig 3. Sectional sliding solidification mould with a diameter of 80 mm for IRSSM: a) general view; b) the shaping section will sleeve.

electrical installation of the sections, thin electrical strips of a heat resisting material are placed in the zone of the induction coil. Glass fibre is used in most cases for this purpose. This is followed by compressing the sleeve using special collars, and the glass tape is mechanically secured between the sections ensuring their electrical insulation.

The channels for the flow of cooling water in the sections are produced by drilling or milling. The first method is technologically simpler: however, in this case, the wall thickness of the section varies resulting in a reduction of the energy transferred to the load.

The milling of the channel is for the flow of water results in the same wall thickness of the sections in the cross-section. Therefore, regardless of the more complicated technology of manufacture of the sleeve, this is economically justified because the efficiency of such a solidification mould is higher. The shaping surface of the sleeve after pressing can be processed in a lathe or ground so that the friction force of the billet during withdrawal can be reduced.

The shaping sleeve of the solidification mould should be produced from deformable metal. It is not recommended to use cast metal components because this type of metal may contain micropores and gas cavities which may cause burning of the solidification mould during melting. Barriers are used to separate the flows of water in the channels of the sections. The material of the barrier should not be electrically conducting to avoid the overflow of induced currents in the sections.

The shaping sleeve is placed in a water collector, and the leaktightness of the joint between the sleeve and the collector is ensured by using sealing rubber rings. The uniformity of the water flow from the collector to the sleeve is

Table 1. Technical characteristics of the sliding solidification moulds for IRSSM

$D_{in.cr}$	$D_{out.cr}$	Height of the working part of the sleeve,	Number of sections, No.	Cooling water flow rate, m^3/h	Special design features
mm		mm			
55	85	70	12	0.8-1.2	Water channels, drilled, diameter 10 mm
68	98	80	12	0.8-1.2	Water channels, milled, size 8 × 8mm
80	110	95	14	1.0-1.5	Water channels, drilled, diameter 10 mm
100	135	120	16	2.0-2.5	Water channels, milled, size 10 × 8mm
150	185	175	16	2.0-2.5	Water channels, drilled, diameter 12 mm

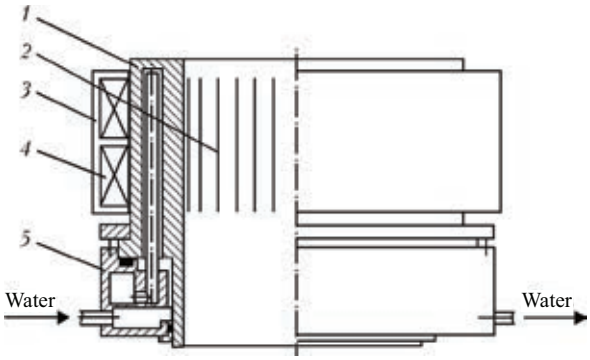

Fig. 4. Principal circuit of the solidification mould for electron beam remelting with a system for electromagnetic mixing [16]: 1) the watercooled copper sleeve; 2) the slits in the zone with the coils; 3) magnetic circuit; 4) electromagnetic coil; 5) the water collector.

ensured by forming a large number of holes in the collector.

The solidification moulds of the same design have been used recently in casting of melting equipment for electron beam melting (Fig. 4). The enable, during melting, the displacement of the metal pool as a result of the effect of electromagnetic coils, powered by the alternating current circuit.

The copper watercooled sleeve of these solidification moulds in the zone of the coils has vertical radial slits, dividing the sleeve into sections. Consequently as a result of the presence of these slits, the electromagnetic field, generated by the coils, penetrates into the internal volume of the solidification mould and results in the mixing of the metal pool.

As a result of electromagnetic mixing in electron beam remelting, the specific consumption of electric energy is almost halved, the melting time decreases and the amount of poured metal is greater [16].

Another variety of the sectional solidification moulds for IRSSM is the solidification mould–ingot moulds in the form of a metal structure with a large amount of metal than the sliding solidification mould, because these moulds are longer than the melted billets. The shaping sleeve of these solidification moulds is collected from the profiled copper pipe with the trapezoidal section (Fig. 5). The application of the profiled pipes greatly simplifies the production of the sections. However, at the wall thickness greater than 2.0–2.5 mm,

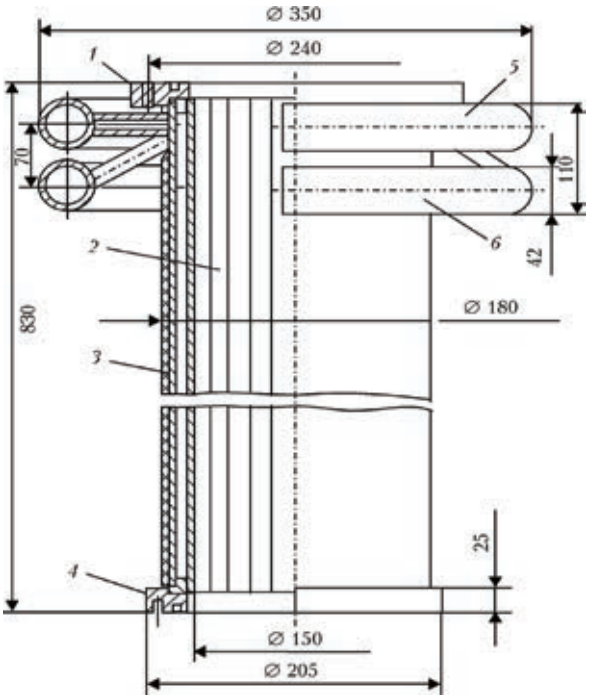

Fig. 5. Design of the sectional solidification mould–ingot moulds with a diameter of 200 mm for melting billets by the IRSSM method (melting equipment OP-151): 1) upper flange; 2) the sections made of the profile copper pipe; 3) the hermetic shell made of glass plastic; 4) the lower flange; 5) the pressure water collector; 6) the discharge water collector.

required for the solidification moulds, calculated for melting large billets, there are problems with the profiling of the pipes.

The sections of the last solidification moulds should be produced by milling long bars to produce the trapezoidal form on the outside and internal channels for the flow of water.

The electrical insulation of the sections is ensured by depositing aluminium oxide on the side contacting walls by thermal spraying or by bonding a glass fibre tape. A flange is welded to the ends of the sleeve on both sides so that the solidification mould can be secured by the upper flange to the melting chamber or the bunker of equipment, and the baseplate is connected with the lower flange. The technical characteristics of the solidification moulds of this type are presented in Table 2.

The water collectors of the initial solidification mould were produced from pipes bent into rings which encircled the sleeve around the perimeter (Fig. 5). The

Table 2. Technical characteristics of the solidification–ingot moulds for IRSSM

D_{cr}, mm	Total height, mm	Number of section, No.	Cooling water flow rate, m^3/h	Special features of design
60	400	16	1.0...1.5	Sectional water collector
80	400	20	1.0...1.8	As above
160	370	24	2.2...2.8	As above
225	800	24	2.5...3.2	Water collector with circular pipes
300	610	28	3.0-4.0	Sectional water collector

supply and removal of water to the section was ensured using copper nozzles, connecting radially between the sections and the collectors.

Changes were made in subsequent designs of the water collectors, and the water supply to the sections is provided without using the radial nozzles and the collectors themselves can be dismantled (Fig. 6a). This greatly simplifies the servicing of the solidification moulds, the external appearance is more aesthetic (Fig. 6b).

To seal the working volume of the solidification mould, the sleeve of the mould is covered along its entire height with a shell made of glass fibre with a thickness of 3.0–3.5 mm produced by winding layers of glass tape with saturation of each layer with an epoxy adhesive. The shell made of the glass parts additional design rigidity and strength to the solidification mould.

The solidification mould of the same design are used in the processes of magnetically controlled electroslag remelting in melting of high-reactivity metals and alloys [17]. As in the case of electron beam remelting, the electromagnetic field, generated by the alternating current in the coil, encircling the sectional sleeve of the solidification mould around the perimeter, penetrates into the internal volume of the solidification mould and causes mixing of the metal pool. This results in averaging of the chemical composition of the metal in the volume of the metal pool and refining of the grains in solidification of the billets.

Recently, induction melting in the solidification mould has been used widely in the production of silicon billets for solar power engineering [18–22]. In France (Emix company) and Japan (Sumko Solar Corporation) companies use induction melting systems which can be used to melt large billets of the multi-crystalline silicon with a cross-section of 400 × 400 mm and up to several metres in length.

These billets are melted in the compound panel solidification mould. Figure 7 shows

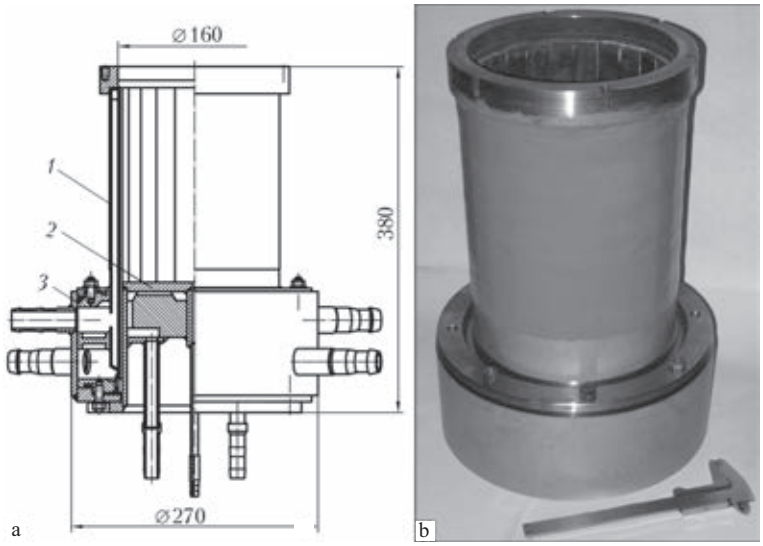

Fig 6. Sectional solidification mould with a sectional water collector: a) in the cross-section; b) general view; 1) the sectional sleeve; 2) the baseplate; 3) the water collector.

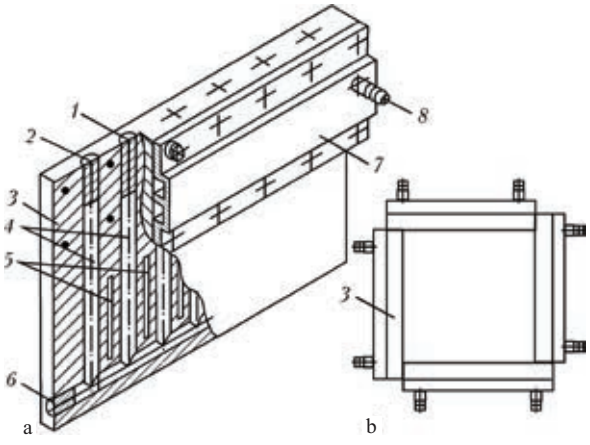

Fig 7. Design of the sectional panel of the assembled solidification mould: a) in the section; b) assembling of the solidification mould: 1, 2, 6) plugs; 3) the copper panel; 4) the channels for the flow of cooling water; 5) the intersectional slits; 7) water collector; 8) the nozzle.

one of the designs of the sectional cooled panel, used for assembling such a solidification mould. The panel in the of the induction coil is divided by slits into vertical sections, with each section containing a channel for the flow of cooling water. All the panels have a quarter collector and, therefore, they can be used to assemble quite easily a solidification mould of the required configuration, in this case of the square cross-section. The solidification mould operates in the hermetic melting chamber of equipment.

Thus, the sectional solidification moulds are very complicated systems as regards the design and the functional possibilities of these moulds are considerably greater than those of the solidification moulds of the conventional design. They are used not only in the shaping of the billets but also in the transfer of energy of the electromagnetic field from the induction coil or other electromagnetic system to the melt which often increases the technical and economic parameters of the remelting processes (for example EBR and ESR), and also the quality characteristics of the remelted metal. Therefore, the range of application of these systems is continuously widening.

References

1. Svenchanskii, A.D., et al., Electrical industrial furnaces. Arc furnaces and equipment for special heating, a textbook, Energoatomizdat, Moscow, 1981.
2. Sapnko, A.I. Mechanical equipment of special electrometallurgy plants, Metallurgiya, Moscow, 1983.
3. Medovar, B.I., et al., Electroslag furnaces, Naukova Dumka, Kiev, 1976.
4. Paton, B.E., et al., Refining remelting, Naukova Dumka, Kiev, 1974, 179–195.
5. Movchan, B.A., In: Welding and special electrometallurgy, Naukova Dumka, Kiev, 1984, 259–264
6. Paton, B.E., et al., Avt. Svarka, 1966, No. 8, 1–5.
7. Bondarchuk, N.I. and Krutyanskii, M.M., Plasma arc melting furnaces, Energoatomizdat, Moscow, 1981.
8. Shippereit, G.H., et al., J. Metals, 1961, No. 2, 140–143.
9. Clites, P.G. and Beall, R.A., US Dept. Interior, 1969, No. 7268, 1–20.
10. Kachur, L.I., Scientific and technical advances, VNIIMI, Moscow, 1987, 65–68.
11. Fomin, I.I., in: Investigations in industrial electric heating, Tr. VNIIETO, Energiya, Moscow, 1981, No. 7, 65–71.
12. Tir, L.L., et al., Elektrotermiya, 11968, No. 73–74, 68–71.
13. Latash, Yu.V., et al., Probl. Spets. Elektrometall., 1986, No. 2, 64–70.
14. Sheiko, I.V., et al., ibid, 1991, No. 3, 76–80.
15. Sheiko, I.V. and Latash, Yu.V., Induction melting with ingot formation in a sectional mould, London, 1999, vol. 11, No. 4.
16. Ladokhin, S.V., et al., Electron beam melting in casting production, Stal', Kiev, 2007.
17. Protokovilov, I.V., Magnetically controlled electroslag melting of multicomponent titanium alloys, E.O. Paton Electric Welding Institute, Kiev, 2006.
18. Basin, A.S. and Shishkin, A.V., Production of Si panels for solar engineering. Methods and technologies. Novosibirsk, 2000.
19.
20. Shkul'kov, A.V., et al., Induktsionnyi nagrev, 2009, No. 3, 16–19.
21. Kaneko, K., et al., in: Photovoltaic Specialists Conf., Kissimmee, vol. 1, 1990, 674–677.
22. Ribeyron, P., et al., in: Proc. Int. Conf. Electromagnetic Processing of Materials, UIE/EPM, Paris, vol. 2, 1997, 303–308.

Submitted 30.9.2011

Advances in Electrometallurgy 2011 ***9*** *(4) 225–233*
Translated from Sovremennaya Elektrometallurgiya 2011 ***9*** *(4) 20–27*

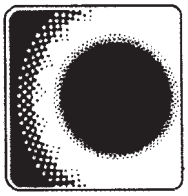

GENERAL PROBLEMS OF METALLURGY

Effect of the thermal cycle of welding on structural transformations in alloys of the Ti–Si–X system

S.V. Akhonin, M.P. Kruglenko, I.K. Petrichenko, E.L. Vrzhizhevskii, R.N. Mishchenko and R.V. Selin

E.O. Paton Electric Welding Institute, Kiev

The formation of the structure in electron beam welding (EBW) of experimental heat-resistant α-, pseudo α-, α+β-alloys with mass fractions of silicon from 0.35 to 3.0 % is studied. In spite of the fact that in alloys, different in silicon content, the amount of particles of silicides of different shapes and sizes differs, similar tendencies in the formation of structure of welded joints in EBW were revealed. In areas of the heat-affected zone (HAZ), where metal was heated below the temperature of polymorphous transformation $T_{p.t}$ the line clusters of particles of silicides, oriented along the rolling direction, were observed for all the alloys. In HAZ areas where metal was heated above $T_{p.t}$ the grain refinement can be observed not only in α-alloys with a high content of silicon but also in α+β-alloy with a low content of silicon. In the weld the grain refinement can be observed both for α-alloys with a high content of silicon, but also for pseudo α-, α+β-alloys with a low content of silicon. Thus, the silicon silicides, contained in these alloys, promote the grain refiningin weld metal and HAZ, blocking the boundaries of growing grains by silicides and manifesting the modifying effect.

The majority of creep-resisting titanium alloys contain silicon which is the most efficient addition for increasing the long-term strength and creep resistance. Even small differences in the content of silicon and other elements in the industrial creep-resisting alloys Ti-1100, IMI-834, VT-18U resulting differences in the properties of the materials and weldability.

In this work, special attention is given to the formation of the structure in electron beam welding (EBW) of the experimental creep-resisting α-, pseudo α-, α+β-alloys with the mass fraction of silicon from 0.35 to 3.0%. The chemical composition of the experimental alloys is presented in Table 1.

Prior to welding, the metal was rolled to a thickness of 6–10 mm by the standard procedure and annealed at 800°C. Welding was carried out in the conditions (U_w = 60 kV, I_w = 80 mA, v_w = 7 mm/s) which is optimum from the viewpoint of preventing cold cracking in welding. The welded joint was cylindrical.

The titanium α-alloys Ti–3.4Si (No. 1), Ti–3.4Zr–2.2Si (No. 2), Ti–1.4 Al–2.9 Sn–6 Zr–3.5 Si (No. 3) with the mass fraction of

Table 1. Chemical composition of the experimental alloys

Alloy No.	Mass fraction of elements, %									
	Al	Sn	Zr	Mo	V	Nb	Si	[O+C+N]	[O]	[N]
1	–	–	–	–	–	–	3.38	0.17	–	–
2	–	–	3.41	–	–	–	2.23	0.22	–	–
3	1.40	2.87	5.95	–	–	–	3.37	0.16	–	–
4	5.64	2.20	3.53	0.43	0.95	–	0.56	–	0.09	0.02
5	5.22	3.33	4.24	0.13	0.61	0.77	0.57	–	0.10	0.02
6	4.29	4.39	5.95	1.57	0.68	4.26	0.35	–	0.24	0.02

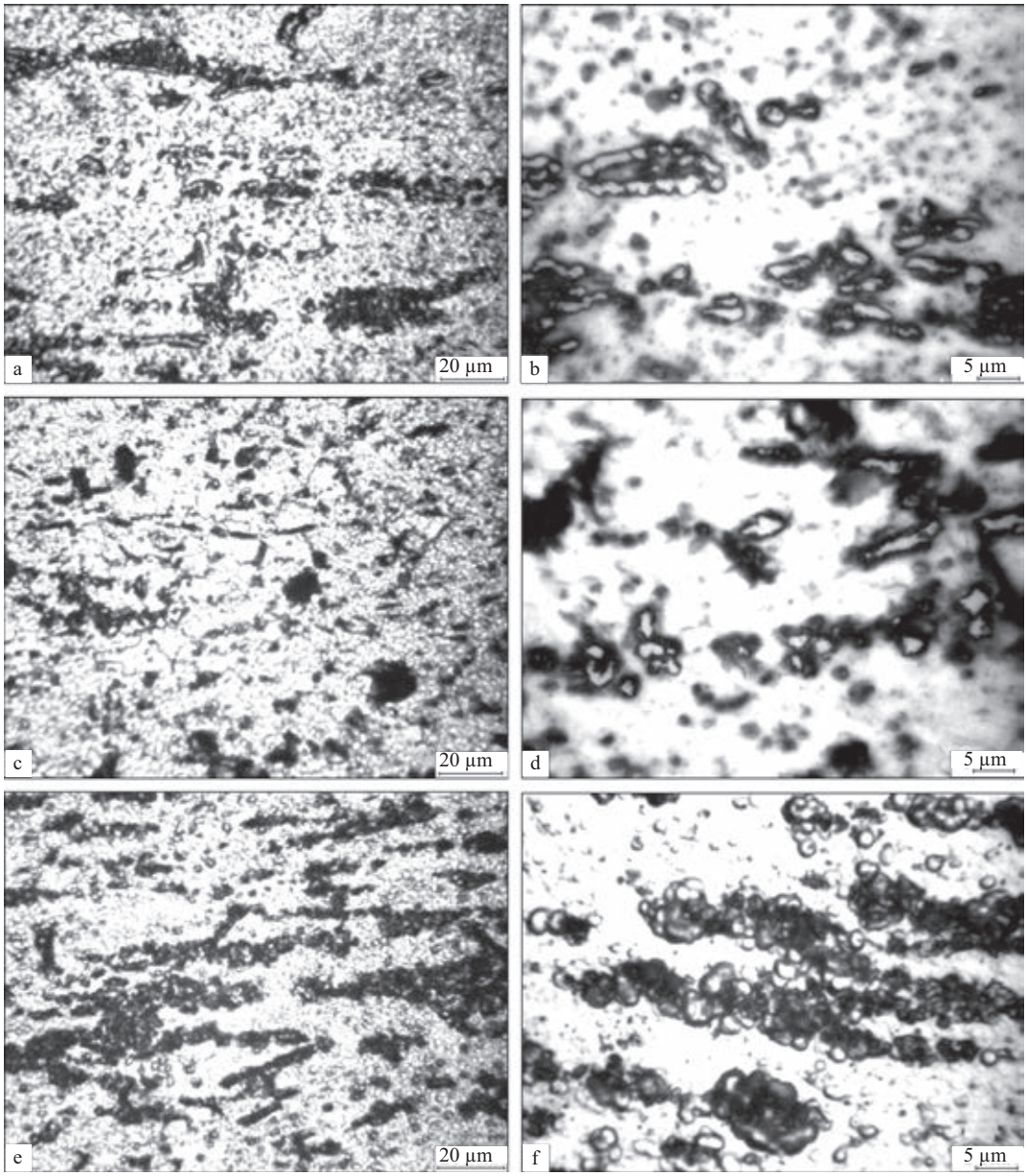

Fig. 1. Microstructure of the parent material of Ti-3.4Si (a, b); Ti-3.4Cr-2.2Si (c, d); Ti-1.4Al-2.9Sn-6Zr-3.4Si (e, f) alloys.

silicon greater than the thermodynamic stable content, were developed at the Institute of Materials Science, National Academy of Ukraine for the working temperatures of 20–700°C [1]. These α-alloys have identical structures not only for the parent metal (PM) but also the welded joints in the weld metal and the heat affected zone (HAZ). The parent metal in the α-matrix contains both uniformly distributed point particles of the silicides and also the silicide particles of larger size, distributed in the form of bands oriented along the welding direction (Fig. 1). All the three alloys contain approximately the same number of the point particles with the size smaller than 1.5 μm. The largest number of the clusters of large particles, reaching 20 μm, was found in the alloy No. 2 (Fig. 1c, d). The largest number of the clusters was found in the alloy No. 3 (Fig. 1e, f). The particles forming these clusters are the smallest (3–5 μm) and have the regular circular shape.

It should also be mentioned that if the silicide particles in the Ti–3.4Si alloy consists only of Ti_5Si_3, then the remaining five alloys contain zirconium and are characterised by the formation of complex silicides with the composition $(Ti, Zr)_xSi$, where x varies in the range 1.67–2.00 [2, 3].

The metal of the welded joints in the α-alloys Ti–3.4Si, Ti–3.4Zr–2.2Si, and Ti–1.4Al–2.9Sn–6Zr–3.4Si alloy has a dendritic structure (Fig. 2). The interdendritic space contain silicides (dark phase). After cooling the weld metal below the polymorphous transformation temperature $T_{p.t.}$ the β→α transformation takes place with the formation of the acicular structure with dendrites. In some areas of the welded joint in the Ti–3.4Si alloy the single fine equiaxed grains with the size of 0.02–0.03 mm, surrounded by silicides (Fig. 2a). The Ti–1.4Al–2.9Sn–6Zr–3.4Si alloy contains a large number of such grains (Fig. 2c). The central part of the welded joint in the Ti–3.4Zr–2.2 Si alloy contains elongated small grains which grew from the fusion zone in the direction normal to the weld axis (Fig. 2b). Annealing of the welded joints at 800°C

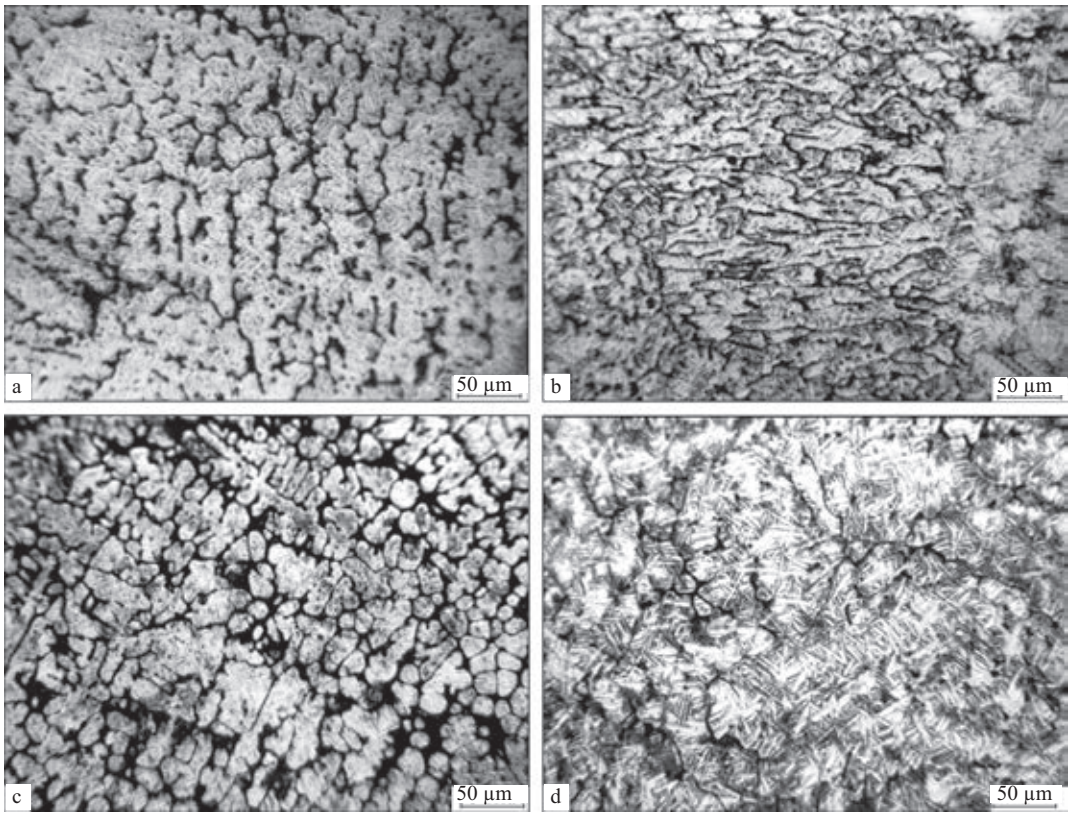

Fig. 2. Microstructure of the weld metal of the α-alloys Ti-3.4Si (a); Ti-1.4Al-2.9Sn-6Zr-3.4Si (c, d); Ti-3.4Zr-2.2Si (b).

for 1 h resulted in the formation of a more distinctive ductile structure of the weld metal for the three alloys (Fig. 2d).

The HAZ metal is characterised by the redistribution and coalescence of the silicides which depend on the temperature to which the area of the HAZ was heated during welding. In heating to temperatures lower than $T_{p.t.}$ and with increase of the distance from the parent metal, the density of the dispersed point inclusions of the silicides decreases whereas the size of the particles forming the bands increases, in comparison with the size in the parent metal.

In heating the metal to the temperatures higher than $T_{p.t}$ the dispersed point precipitates of the silicides in the volume of the grains are minimum and distributed mainly in the form of bands elongated in the welding direction of the parent metal. The metal of the weld zone of the HAZ shows the formation of groups of small equiaxed grains with the size of 0.02–0.03 mm (Fig. 3).

On approach to the welded joint the degree of refining of the grains increases, in contrast to the welded joints in the majority of the titanium alloys, where the maximum grain size in the HAZ metal was recorded in the vicinity of the fusion zone [4].

Of the three alloys investigated, the lowest degree of refining of the grains was recorded in the Ti–3.4 Zr–2.2Si alloy (Fig. 3c), the highest in the Ti–1.4Al–2.9Sn–6Zr–3.4Si alloy (Fig. 3b). In cooling of the HAZ metal, heated to the temperatures in the β-the region, at temperatures below $T_{p.t.}$ the $\beta \rightarrow \alpha'$ transformation takes place with the formation of an acicular α'-phase, as in the welded joint. After cooling of the welded joints, the plate-shaped structure in the HAZ metal, similar to the weld metal, becomes more distinctive (Fig. 3d).

Thus, the silicon silicides, present in this alloys, result in the refining of the grain in the weld metal, especially in the HAZ, blocking the boundaries of the growing grains by the

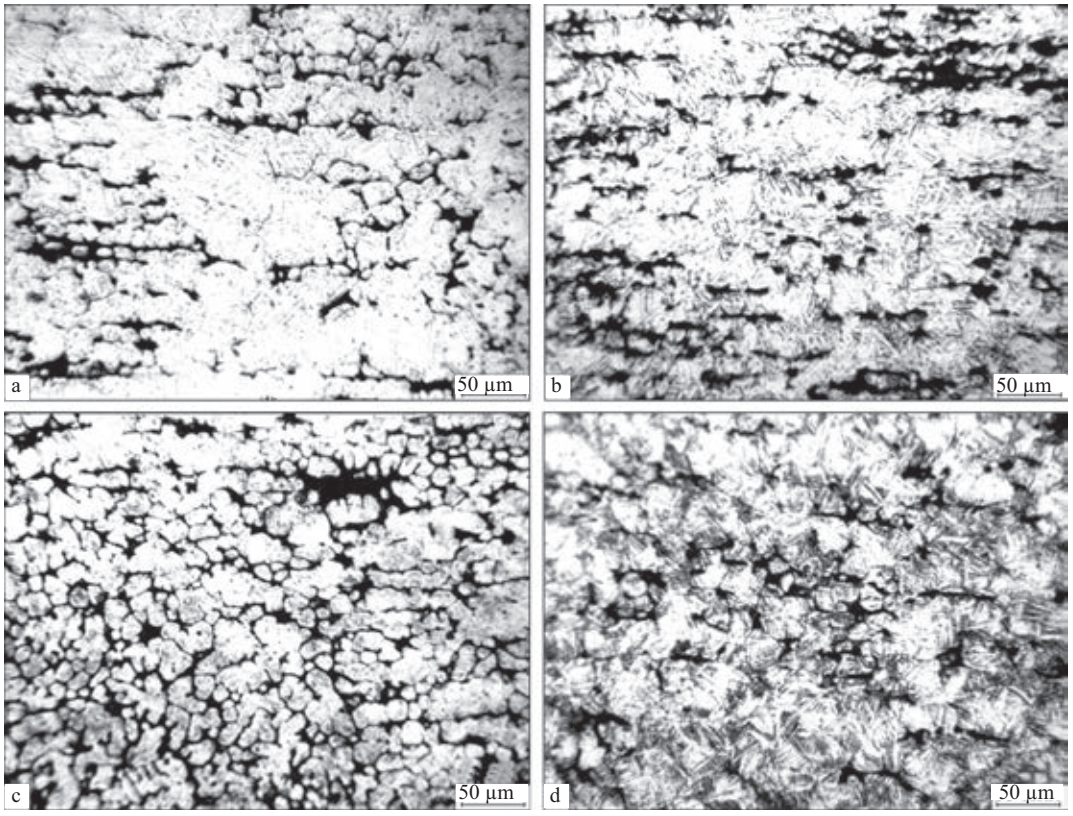

Fig. 3. Microstructure of the HAZ metal in the weld zone of the α-alloys Ti-3.4Si (a); Ti-3.4Zr-2.2Si (b); Ti-1.4Al-2.9Sn-6Zr-3.4Si (c, d).

silicides and showing the modifying effect.

The Ti–5.6 Al–2.2 Sn–3.5Zr–0.4Mo–1V, 0.6 Si (No. 4) and Ti–5.2Al–3.3Sn–4.2Zr–0.1Mo–0.6V–0.8Nb–0.6Si (5) alloys belongs to the group of the pseudo α-alloys of titanium.

The coefficient of stabilisation of the β-phase k_β for the alloy No. 4 is equal to 0.1 and for the No.5 alloy it is 0.07. The Ti–5.6Al–2.2Sn–3.5Zr–0.4Mo–1V, 0–6Si alloy differs from the Ti-1100 alloy by the presence of a small amount of vanadium (0.95 wt.%), the Ti–5.2Al–3.3Sn–4.22Zr–0.1Mo–0.6V–0.8Nb–0.6Si alloy differs from IMI-834 alloy by the mass fractions of aluminium 0.28 and of molybdenum 0.12% lower than the minimum values, and also by the presence of vanadium (0.61%).

In the condition after rolling, the alloys No. 4 and 5 contain a plate-shaped structure in which the silicide particles are distributed quite uniformly at the boundaries of the primary beta β-grains (Fig. 4a–c). After annealing, the dispersed particles of the silicides are distributed mostly along the boundaries of the α-plates (Fig. 4e).

The microstructure of the weld metal of the Ti–5.6Al–2.2Sn–3.5Zr–0.4Mo–1V–0.6Si alloy consisted of the primary β-grains, elongated in the direction of heat removal, and the plate shaped α-phase in the volume of the grains. After welding, the particles of the silicides are randomly localised both at the boundaries of the β-grains and in the volume of the grains (Fig. 5a, b).

The Ti–5.2Al–3.3Sn–4.2Zr–0.1Mo–0.6V–0.8Nb–0.6S also consists of the primary β-grains, elongated in the direction of heat removal, with the plate-shaped α′-phase in the volume of the grains. However, the equiaxed grains form in this alloy along the weld axis (Fig. 5c). After annealing of these pseudo-α-alloys of titanium, the silicide particles are localised mainly at the boundaries of the α-plates or primary β-grains (Fig. 5d).

The microstructures of the HAZ metal of the welded joints in the experimental alloy Ti–5.6Al–2.2Sn–3.5Zr–0.4Mo–1V–0.6Si and Ti–5.2Al–3.3Sn–4.2Zr–0.1Mo–0.6V–0.8Nb–0.6Si alloys do not differ greatly. The metal of the weld zone of the HAZ is characterised by the formation of the large equiaxed β-grains (Fig. 6a).

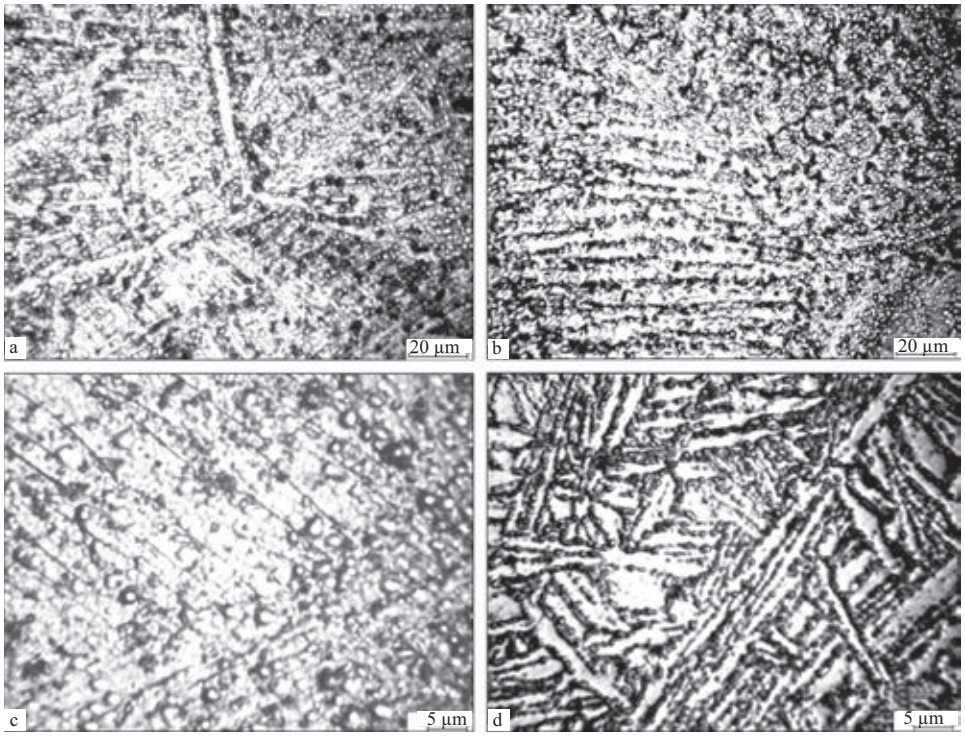

Fig. 4. The microstructure of the parent metal of the Ti- 5.6Al-2.2Sn-3.5Zr-0.4Mo-1V-0.6Si (a, c, d); Ti-5.2Al-3.3Sn-4.2Zr-0.1 Mo-0.6V-0.8Nb-0.6Si (b).

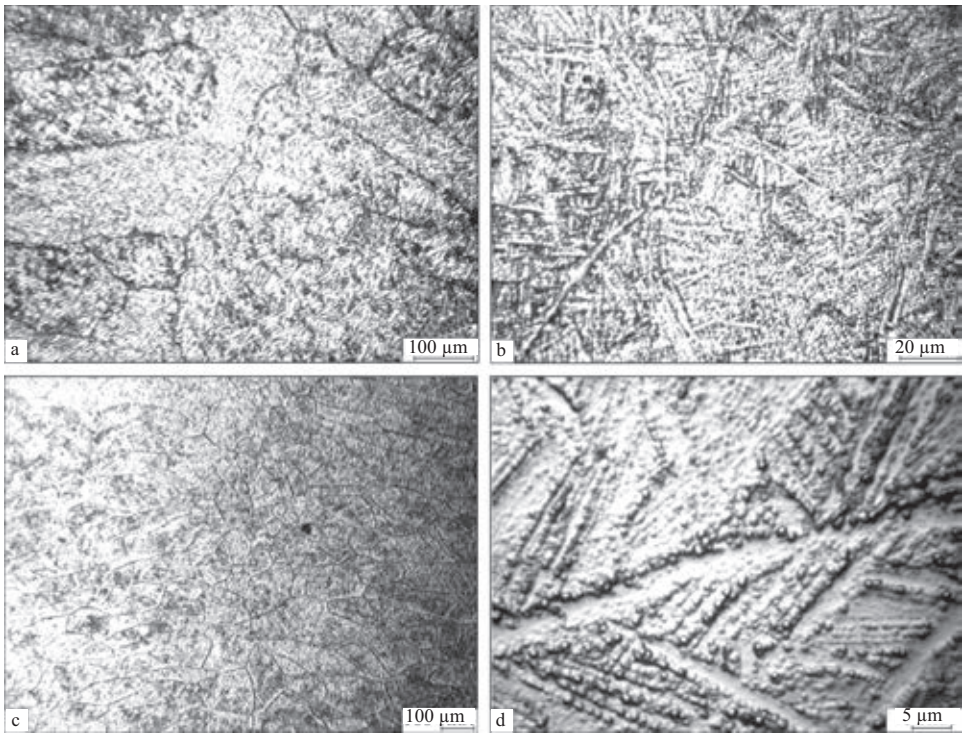

Fig. 5. The microstructure of the weld metal of the Ti-5.6Al-2.2Sn-3.5Zr-0.4Mo-1V-0.6Si (a, d); Ti-5.2Al-3.3Sn-4.2Zr-0.1Mo-0.6V-0.8Nb-0.6Si (c,b) alloys.

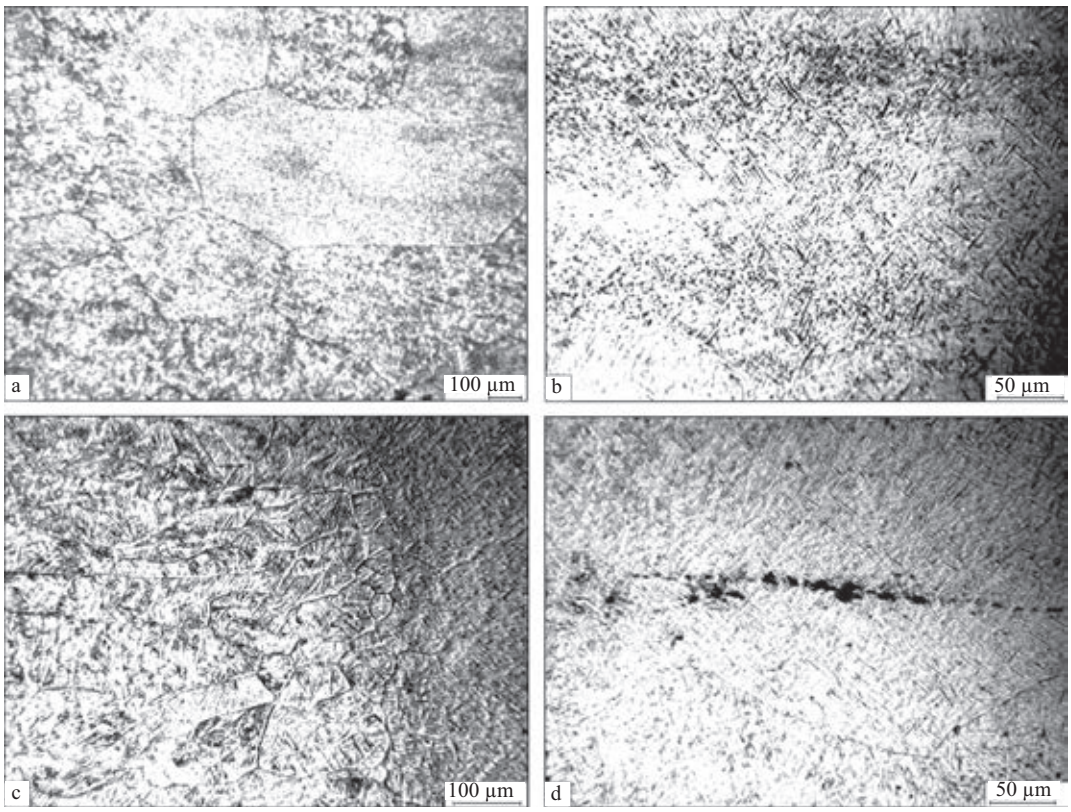

Fig. 6. The microstructure of the HAZ of the Ti-5.6Al-2.2Sn-3.5Zr-0.4Mo-1V-0.6Si (a, b); Ti-5.2Al-3.3Sn-4.2Zr-0.1Mo-0.6V-0.8Nb-0.6Si (c,d) alloys.

In cooling to temperatures below $T_{p.t.}$ the volume of the primary β-grains, like the weld metal, is characterised by the occurrence of the β→α transformation with the formation of the plate shaped α′-phase whose properties are similar to those of the α-phase. The section of the HAZ metal, heated to temperatures below $T_{p.t.}$ It is also characterised by the formation of the plate shaped α′-phase. The HAZ contains bands of point precipitates of silicides, elongated in the direction of welding the metal in the direction normal to the welded joint (Fig. 6b, d). After annealing, the silicides usually decorate the boundaries of the α-plates.

In all pseudo-α-alloys of titanium the size and number of the resultant silicides suppose the modification effect and delayed the growth of the β-grains in the weld metal and the weld zone, as recorded in the α-alloys with a large amount of silicon. However, in the Ti–5.2Al–3.3Sn–4.2Zr–0.1Mo–0.6V–0.8Nb–0.6Si small equiaxed β-grains (Fig. 6c) still appear along the axis of the welded joint.

The Ti–4.3Al–4.4Sn–6Zr–1.6Mo–0.7V–4.3Nb–0.4Si alloy (No. 6) belongs to the titanium α+β alloys of the martensitic type, and its k_{β} value is equal to 0.31. The microstructure of the alloy is shown in Fig. 7. After rolling, disintegration and spheroidisation of the plate shaped structure take place (Fig. 7a–f), and a fine plate shaped structure again forms after annealing (Fig. 7d). In the direction along the rolling direction there are band-like precipitates of finely dispersed particles silicides [5], regardless of the fact that the silicon content of this alloy is in the range of its solubility in the α-phase. Aluminium decreases the already low solubility of silicon in the α-titanium [6].

The metal of the welded joint of the experimental alloy Ti–4.3Al–4.4Sn–6Zr–1.6Mo–0.7V–4.3Nb–0.4Si consists of the primary β-grains of different shapes. The upper part of the welded joint is characterised by the formation of the largest grains, elongated in the direction of heat removal under the angle of 45–60° in relation to the axis of the

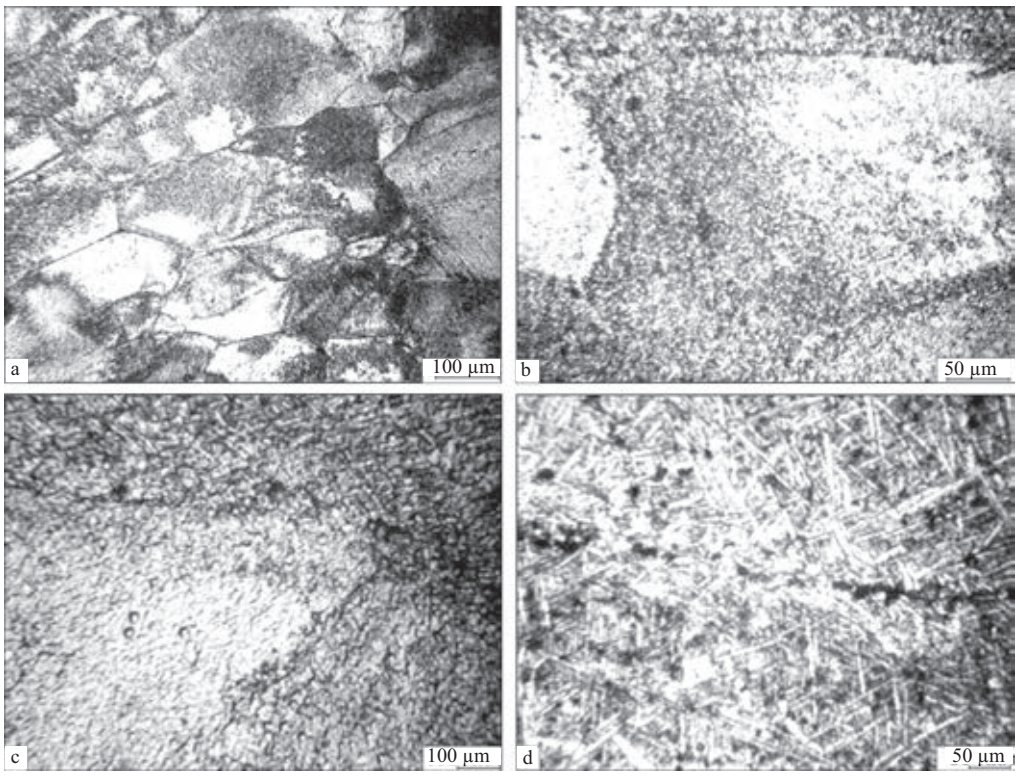

Fig. 7. The microstructure of the experimental alloy Ti-4.3Al-4.4Sn-6Zr-1.6Mo-0.7V-4.3Nb-0.4Si (here and in Fig. 8 and 9 the notations a-d are explained in the text).

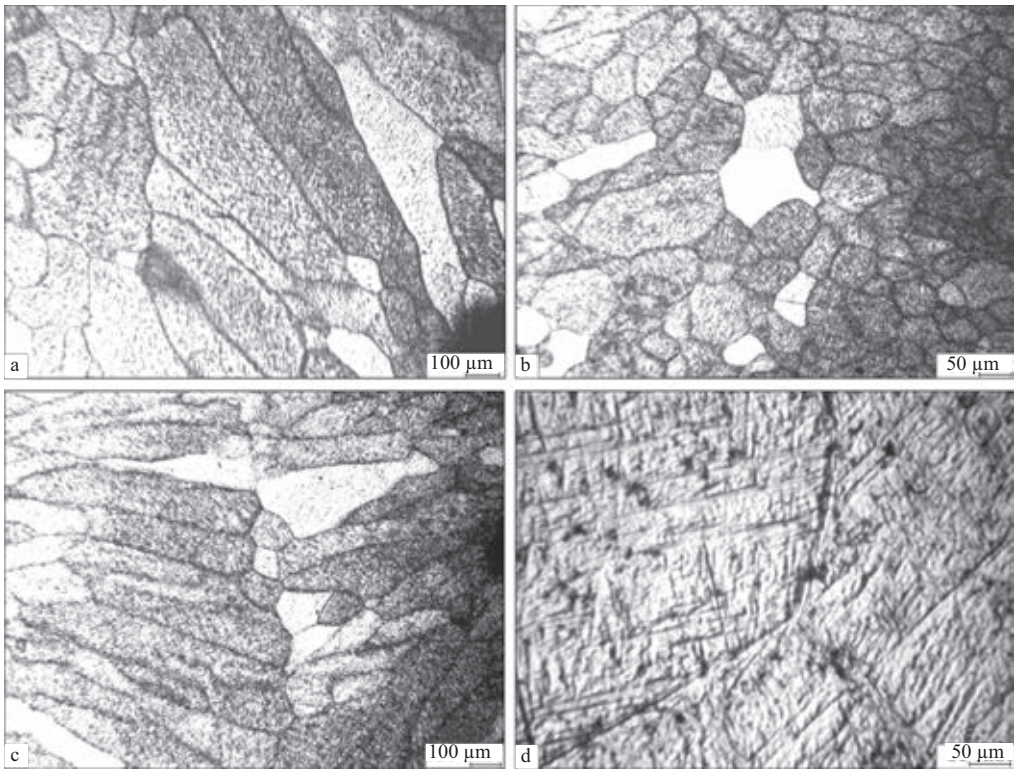

Fig. 8. The microstructure of the weld metal of the welded joint in Ti-4.3Al-4.4Sn-6Zr-1.6Mo-0.7V-4.3Nb-0.4Si alloy.

welded joint (Fig. 8a). The central part of the welded joint is characterised, almost throughout the entire width of the welded joint, by the formation of equiaxed polyhedral grains, considerably finer than in the upper part of the welded joint (Fig. 8b). Closer to the weld root the elongated grains merge under the angle of approximately 180° (Fig. 8c). The shape and size of the primary β-grains are greatly affected by the welding conditions. The metastable martensitic β′-phase forms in the volume of the primary grains. On the background of the needle-shaped structure, there are finely dispersed particles of the silicides which are distributed both at the boundaries of the grains and inside them (Fig. 8d).

In the metal of the HAZ of the welded joint in the Ti–4.3Al–4.4Sn–6Zr, 1–6 Mo–0.7V–4.3Nb–0.4Si alloy there are three structurally different areas. The weld zone consists of the equiaxed polyhedral primary β-grains with the acicular morphology of the intragranular α′-phase (Fig. 9a). Further away from the welded joint there is the area of the HAZ in which partial recrystallisation took place with the formation of fine equiaxed grains (Fig. 9b). Alongside the parent metal there is the region of the HAZ heated to temperatures lower than $T_{p.t.}$ and the recrystallisation temperature, and follows the structure of the parent metal. The second and third regions of the HAZ contained banded of point formations of the silicides (Fig. 9c).

It should be mentioned that these bands are the areas of the formation of the fine equiaxed grains. Similar structures are also found in the alloys with a high silicon content. In some local areas of the HAZ fine equiaxed grains surrounded by the eutectics appeared (Fig. 9d).

Thus, regardless of the fact that the alloys of different types with the different silicon content are characterised by the formation of different amounts of the silicide particles of different shape and dimensions, there are identical tendencies in the formation of the structure of the welded joints in electron beam welding. In the areas of the HAZ where the metal was heated to temperatures lower than the polymorphous transforma-

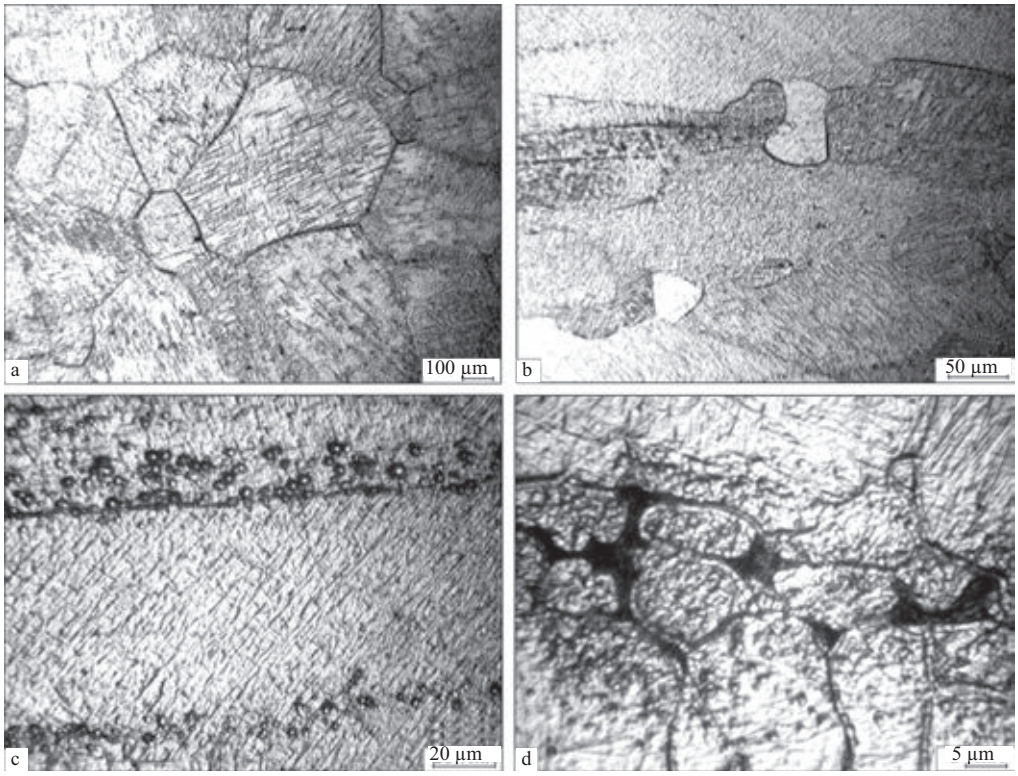

Fig. 9. The microstructure of the HAZ of the welded joint in Ti–4.3Al–4.4Sn–6Zr–1.6Mo–0.7Vi–4.3Nbi–0.4Si alloy.

tion temperature $T_{p.t}$, all the alloys showed point-shaped clusters of the silicide particles, oriented along the rolling direction. In the areas of the HAZ in which the metal was heated above $T_{p,t.}$ examination showed grain refining not only in the α-alloys with a high silicon content but also in the α+β-alloy with a low silicon content. The weld metal also showed refining of the grains for both the α-alloys with the high silicon content and also for the pseudo α-, α+β-alloys with a low silicon content. Thus, the silicon silicides, present in these alloys, support refining of the grains in the weld metal and the HAZ, blocking the boundaries of the growing grains and exerting the modification effect.

References

1. Firstov, S.A., in: Int. Conf. Science for materials in the frontier of centuries. Advances and Challenges, Kiev, 2002, 623–624.
2. Anoshkin, N.F. and Sigalov, Yu.M., Tekhnol. Legkikh Splavov, 2002, No. 1, 38-50.
3. Singh, A.K. and Ramachandra, C., Journal of Materials Science, 1997, No. 32, 229–234.
4. Grabin, V.F., Fundamentals of physical metallurgy and heat treatment of welded joints in titanium alloys, Naukova Dumka, Kiev, 1975.
5. Firstov, S.A., et al., Obshch. Vopr. Metall., 2006, No. 2, 33–38
6. Kornilov, I.I. and Budberg, P.B., Equilibrium diagrams of binary and ternary systems, VINITI, Moscow, 1961, 78–81.

Submitted 5.7.2011

Advances in Electrometallurgy 2011 ***9*** *(4) 234–238*
Translated from Sovremennaya Elektrometallurgiya 2011 ***9*** *(4) 28–31*

Special features of the structure of an intermetallic alloy after zone recrystallisation

N.V. Piskun, I.L. Bogaichuk, E.A. Asnis, G.M.Grigorenko, I.I. Statkevich, V.V. Lakomskii, V.A.Kostin, R.V. Kozin and V.A. Berezos

EO .P aton Electric Weld ng Institute,K iev

The effect of zonal recrystallization of intermetallic alloy of Ti–Al–Nb–Zr–Cr system on structure and some mechanical characteristics of the alloy was investigated. It was found that the zonal remelting promotes the formation of directed crystallization, decrease in size of intermetallic grains, reduction in its hardness and more uniform distribution in the cross section and volume of ingots as compared with intermetallics, produced by the method of electron beam cold hearth melting (EBCHM). These structural changes increase the strength and ductility of intermetallics.

The intermetallic alloys of the Ti–Al system are characterised by the unique structural properties and are regarded as highly promising alloys for components for aerospace technology. In addition to the high values of creep strength, heat resistance and corrosion resistance, these alloys have also low density (3.8–4.0 g/cm^3) so that one of the most important requirements on the components for aerospace technology – a large reduction of the weight of the structures – can be satisfied.

The main shortcoming of these alloys is the low plasticity at room temperature which complicates technological processing and industrial application. Therefore, the development of the alloys of the Ti–Al system and of the methods of production of these alloys with the optimum combination of the high-temperature and low-temperature properties is a very urgent task.

The mechanical properties of titanium aluminide are strongly affected by their composition and structure.

In this study, investigations were carried out into the structure and some mechanical properties of the intermetallic alloy of the Ti–Al system with the following composition, wt.%: Ti 46.5; Al 35; Nb 12.5; Zr 3; Cr 3, developed at the E.O. Paton Electric Welding Institute, Kiev and produced by the methods of electron beam cold hearth melting (EBCHM) [1].

Figure 1 shows the microstructure of the initial material melted by the ECHM method which consists of large, slightly elongated grains with no distinctive boundaries. The grain size was 40–45 μm. The body of the grains con-

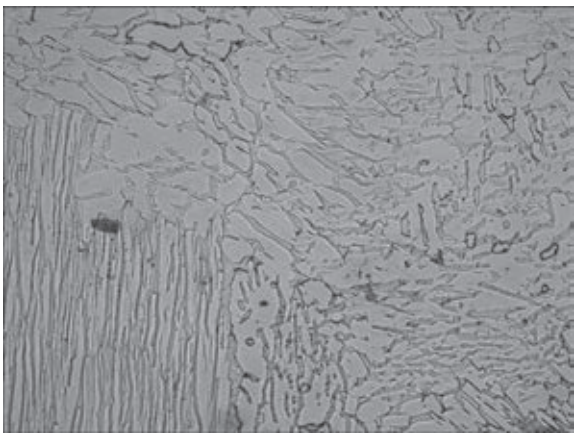

Fig. 1. Microstructure (× 320) of the intermetallic alloy after electron beam cold hearth remelting.

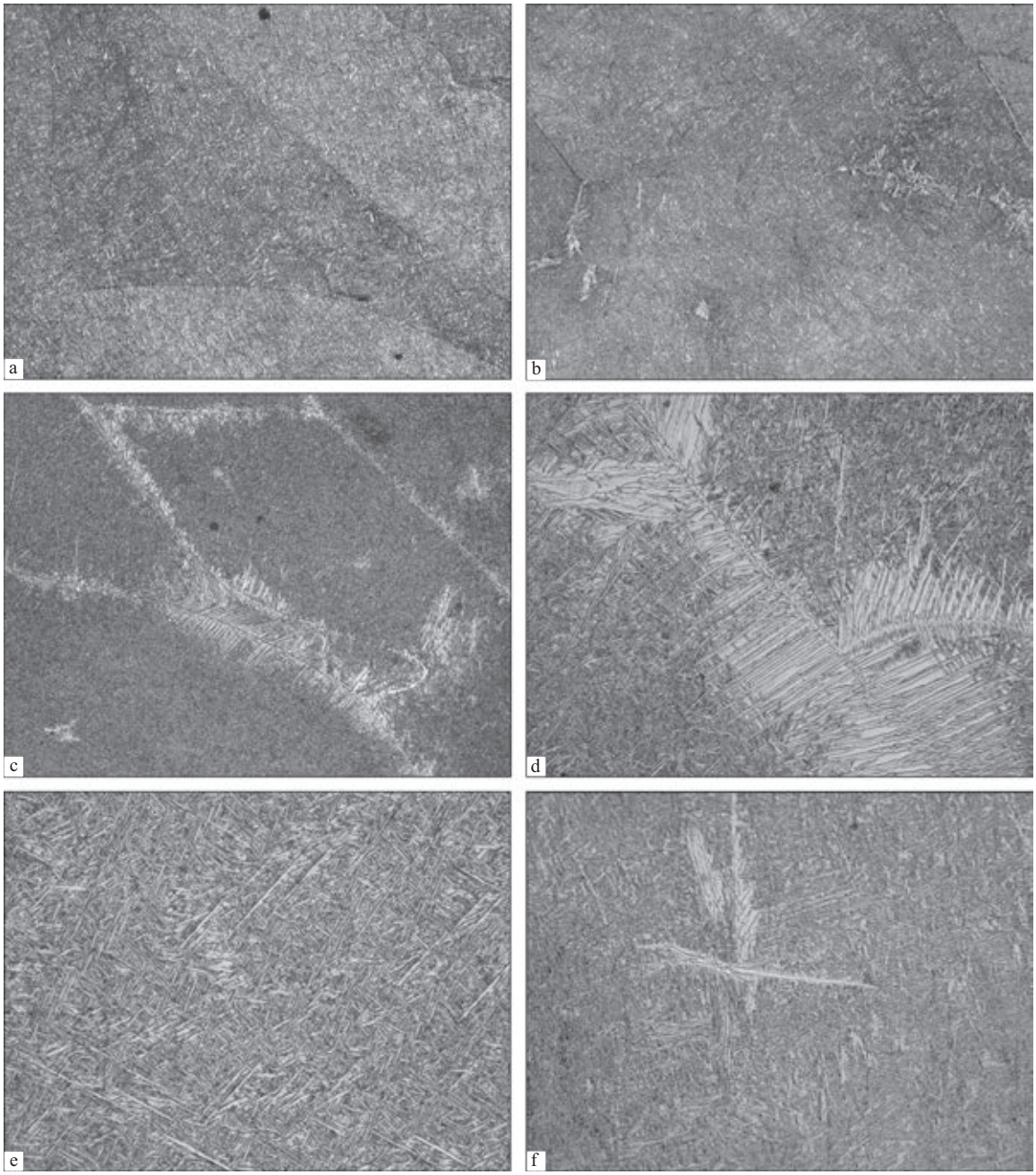

Fig. 2. Microstructure of the intermetallic alloy after zone recrystallisation: a) beginning, × 80; b) middle, × 80; c) end of the melting process, × 80; d) the fragment of the grain with the martensite-like needles, × 320; e) the three-phase structure inside the grain, × 500; f) the section of the grain with the precipitates of the β- and -phase, × 320.

tained the lamellar structure of the γ-phase and a fine acicular α_2-phase. The hardness of the intermetallic compound was measured in LECO equipment at a load of 25 g. The hardness of the material of the grains varied from 2372 to 3110 MPa. The areas with the precipitates of the acicular phase which on the equilibrium diagram was identified as $\gamma+\alpha_2$, showed higher values of the hardness (from 5140 to 6270 MPa).

In the subsequent stage of the experiments, the alloy was subjected to zone recrystallisation. The application of zone melting ice of possible to produce directional crystallisation

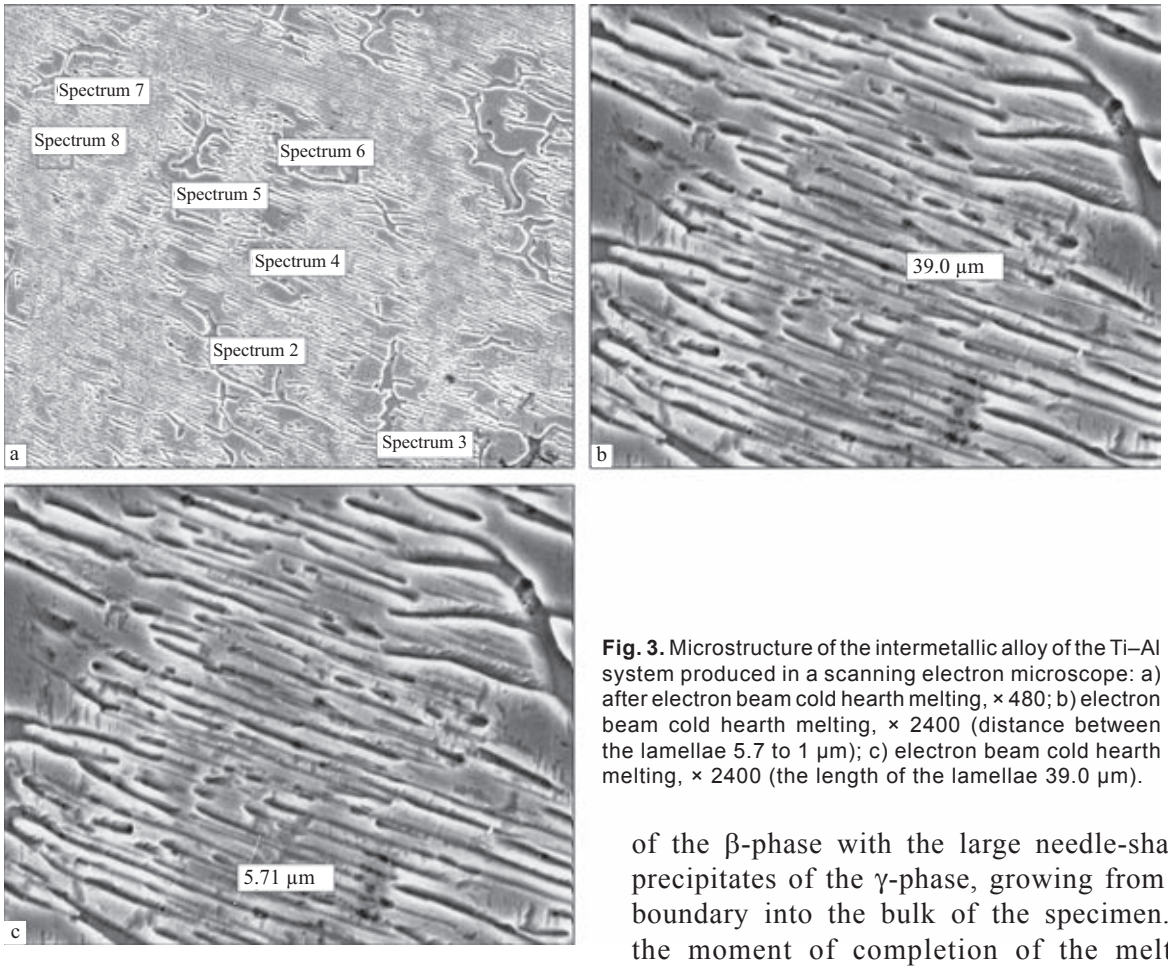

Fig. 3. Microstructure of the intermetallic alloy of the Ti–Al system produced in a scanning electron microscope: a) after electron beam cold hearth melting, × 480; b) electron beam cold hearth melting, × 2400 (distance between the lamellae 5.7 to 1 μm); c) electron beam cold hearth melting, × 2400 (the length of the lamellae 39.0 μm).

[2]. In the case of the efficiently selected melting technology, the solidification front is almost flat. This results in the more uniform distribution of the impurities throughout the cross-section and the volume of the ingot and also reduces the level of the stress state and, correspondingly, the plasticity of the material is higher.

The microstructure of the specimen after zone remelting (Fig. 2) consists of the grains elongated in one direction with the mean size of 31.5 μm which are also characterised by the presence of an internal lamellar structure consisting of the ($\gamma+\alpha_2$) plate shaped colonies. In the centre of the specimen (Fig. 2a) the boundaries between the grains are thin, with a thickness of 2 μm. As the zone moves in the direction of the upper part of the specimen, the grain boundaries become thicker (Fig. 2b) and contain the precipitates of the bright layers of the β-phase with the large needle-shaped precipitates of the γ-phase, growing from the boundary into the bulk of the specimen. At the moment of completion of the melting process, the thickness of the grain boundaries with the large martensite-like needles in the light matrix (Fig. 2c) was 5–12 μm. A fragment of this structure is shown in Fig. 2d. A three-phase structure (Fig. 2e) [3] appears inside the grains at the end of melting and consists of the γ-phase with the thick needles, the β-phase and the fine dispersion particles of the α_2-phase.

In addition to this, inside some grains there are areas of the light precipitate of the β-phase with the thick γ-needles (Fig. 2e).

The distribution of the hardness in the specimens of the intermetallic compound after zone recrystallisation was also determined. The experimental results show that the hardness, measured with a step of 1 mm along the section, was stable and its mean value was 4640 MPa, and the hardness inside the grain was the same as that at the grain boundary. This was almost 20% lower than in the alloy melted by the EBCHM method.

Table 1. Chemical composition of the titanium aluminide alloy after electron beam cold hearth melting, determined by the methods of quantitative x-ray spectrum microanalysis at different points of the investigated specimen

Spectrum No.	Mass fraction of elements, %				
2	18.40	59.71	8.89	1.56	11.45
3	22.18	59.92	4.59	3.21	10.09
4	30.17	52.57	1.74	3.98	11.55
5	29.96	51.88	2.06	5.05	11.05
6	19.89	59.44	8.90	1.13	10.65
7	27.07	56.10	2.72	3.71	10.39
8	29.63	55.86	2.61	2.89	9.02

Table 2. The chemical composition of the titanium aluminide alloy after zone recrystallisation, determined by quantitative x-ray spectrum microanalysis at different points of the investigated specimen

Spectrum No.	Mass fraction of elements, %				
1	29.81	52.81	1.66	3.62	12.10
2	28.36	54.68	2,64	3.01	11.31
3	26.46	54.77	4.22	2.76	11.79
4	28.07	55.60	2.11	2.50	11.71
5	27.88	53,27	2.68	3.09	13.09
6	27.84	55.76	2.56	3.40	10.43
7	23.51	55.97	6.23	4.36	9.94
8	25.70	55.46	4.00	3.59	11.25

The structure was studied in a JSM-840 scanning electron microscope with x-ray spectrum microanalysis of the specimens in the initial condition after EBCHM and subsequent zone recrystallisation.

Figure 3a shows the microstructure of the alloy. The characteristic points were investigated by quantitative x-ray spectrum microanalysis (Table 1). The analysis results show that the light areas are enriched with niobium which is a β-stabiliser [4]. Thus, it may be assumed that the light phase is the β-phase. The mean length of the lamellae was also determined, 39.0 μm (Fig. 3b) and the distance between them was 5.7 μm (Fig. 3c).

Figure 4a shows the microstructure of the specimens of the intermetallic alloys subjected to zone recrystallisation. The figure shows that the zone remelting and results in the formation of the structure elongated in the direction of movement of the zone and district increase the plasticity of the material [5]. The distribution of the elements in the field of the specimen was relatively uniform and corresponded to the stoichiometric composition of the alloy (Table 2).

At a magnifications of 2400, as in the case of the specimens of the initial material, the distance between the lamellae was determined (Fig. 4b). Since the material after zone remelting is characterised by the formation of the lamellar structure, consisting of the long continuous lamellae, elongating along the direction of movement of the zone, it was not possible to determine the size of these grains. The distance between the lamellae was 4.67 μm which was 18% smaller than

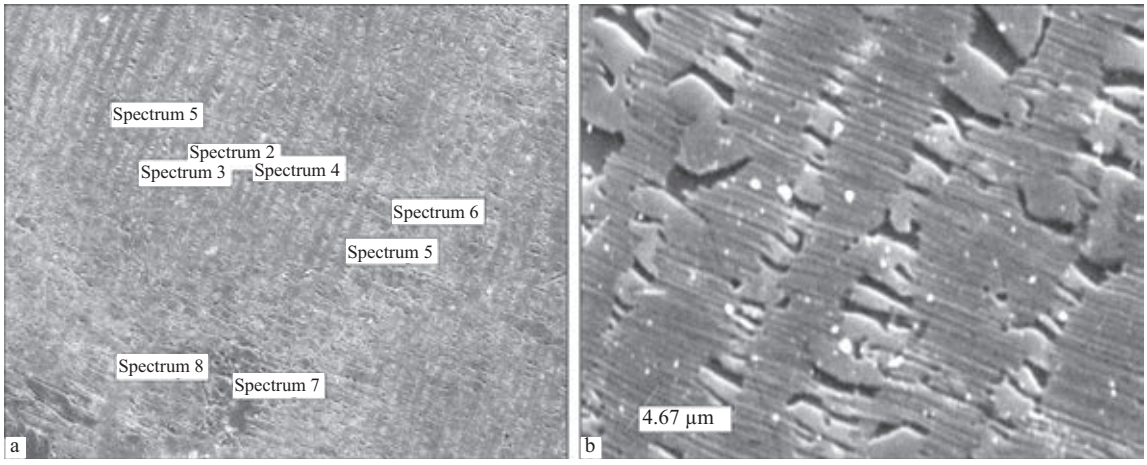

Fig. 4. Microstructure of the Ti–Al intermetallic alloy after zone recrystallisation: a) × 480 (scanning electron microscope); b) × 2400 (scanning electron microscope, the distance between the lamellae 4.67 μm).

in the case of the parent material.

It was shown in [6] that the plasticity values depend mostly on the type of structure, and the mechanical characteristics of the intermetallic alloys, with the lamellar structure, depend to a greater extent on the ratio between the length of the lamellae and the distance between them. At the optimum combination of the parameters of the plate-shaped structure, the plasticity of these alloys maybe similar to that of the globular structure.

The mechanical tests with uniaxial tensile loading at the room temperature show that the strength of the intermetallic alloy after zone melting was 580 MPa, and the relative elongation 2.2%, whereas the strengths of the parent material was 524 MPa, relative elongation 0.8%.

Thus, the experiments show that the zone recrystallisation of the intermetallic alloy of the Ti–Al–Nb–Zr–Cr alloy, produced by the EBCHM, results in directional solidification, the reduction of the grain size of the intermetallic compound, reduction of hardness and the more uniform distribution of the hardness value in the cross-section on volume of the ingot. This increases the strength and plasticity of the intermetallic alloy and has been confirmed by the results of mechanical tests.

References

1. Zhuk, G.B., et al., Sovremennaya Elektrometallurgiya, 2003, No. 4, 20–22.
2. Pfann, V., Zone melting, Mir, Moscow, 1970.
3. Imaev, V.M., et al., Fiz. Met. Metalloved., 2008, vol. 105, No. 5, 516–522.
4. Povarova, K.B., et al., Metally, 1998, No. 3, 31–41.
5. Kuznetsov, A.V., et al., ibid, 2002, No. 6, 102–110.
6. Titanium alloys. The composition, structure, properties, a Handbook, The scientific Research Institute of Light Alloys, Moscow Institute ofTechnology, 2009, 466–468.

Submitted 24.3.2011

Advances in Electrometallurgy 2011 ***9*** *(4) 239–250*
Translated from Sovremennaya Elektrometallurgiya 2011 ***9*** *(4) 32–41*

Magnetohydrodynamic technologies in metallurgy (review)

I.V. Protokovilov

EO .P aton Electric Weld ng Institute,K iev

Examples of application of magnetohydrodynamic (MHD) effects in metallurgical processes are given. The tasks of application of electromagnetic effects are shown, and the classification and principle of operation of main MHD-devices are described.

Introduction

Metallurgy is traditionally one of the main branches of the magnetohydrodynamic (MHD) effects. This is due to the presence in metallurgical furnaces of larte volumes of conductive liquids – molten metals and slags. At the same time taking into account the specificity of steel production (high temperatures and aggressive environments) this often requires the use of contactless force action on melts to solve various technological problems, as well as management of the properties of melted metal. These effects can be realized through the use of electromagnetic forces.

Work on the creation of metallurgical MHD technologies have been actively carried out since the beginning of 1960s. Now they have been widely developed and have found practical applications in various metallurgical processing stages: during transportation and dosage of iron and steel melts for the intensification of heat and mass transfer in aggregates melting, refining of metals and alloys, control of the crystallization of ingots, etc. (Fig. 1) [1–5].

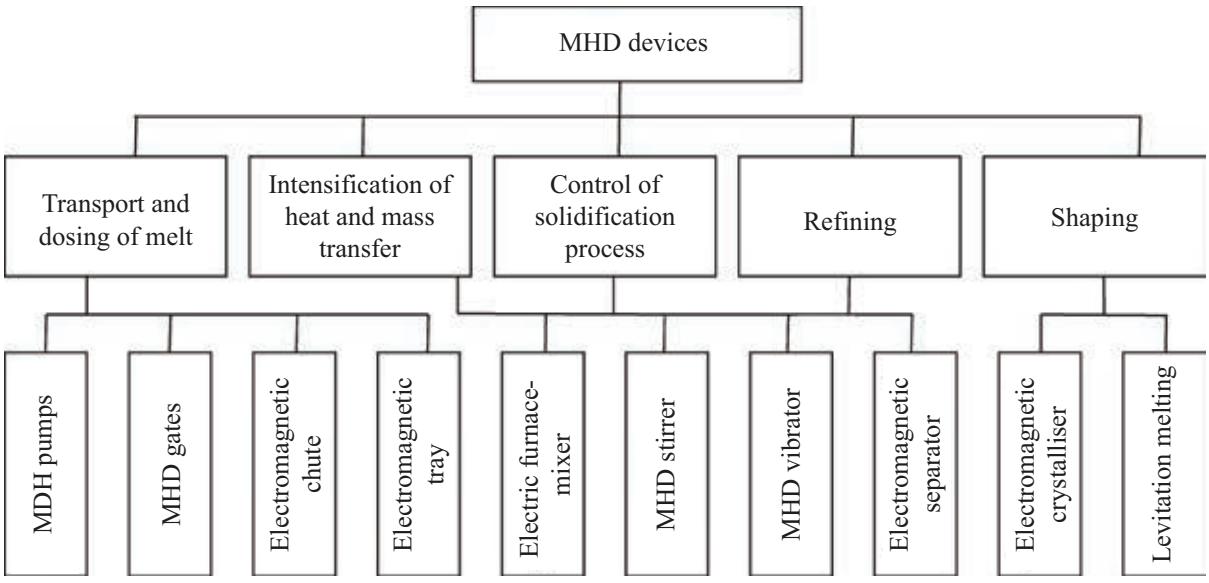

Fig. 1. Purpose and types of metallurgical MHD devices.

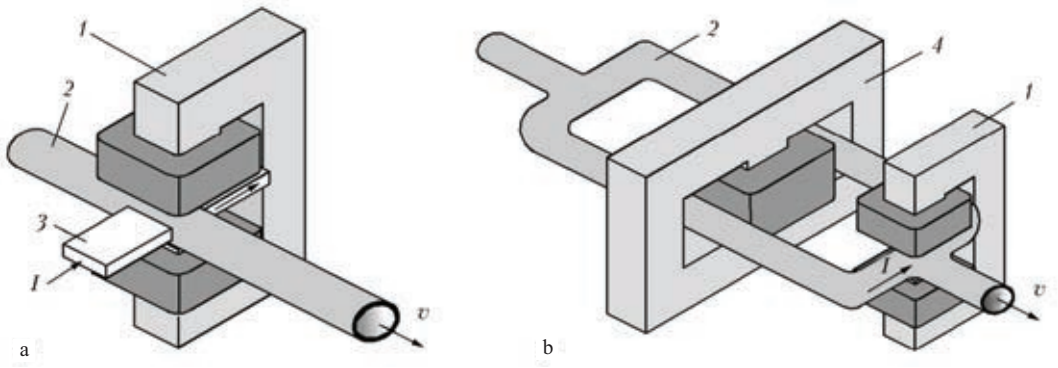

Fig. 2. Schematic diagram conduction (a) and induction, transformer type (b) MHD pumps: 1 - electromagnet, 2 - channel; 3 - current lead; 4 - coil; I - current; v - velocity of the melt,

The principle of operation of most metallurgical MHD devices is based on the interaction of the produced external magnetic field with the electric current flowing in a current-carrying liquid (molten steel). As a result of such interactions three-dimensional electromagnetic forces, leading to a force on the fluid, occur in a liquid medium. The value and direction of these forces is determined by the vector product of the magnetic field and current density in the melt. Accordingly, the greatest electromagnetic forces are important in the case when the vectors of the magnetic field and current are mutually perpendicular (so-called crossed fields).

It should be emphasized that all the metals in the molten state are practically nonmagnetic and for the use of elektromagnetic force it is important that the medium is conducting.

According to the method of generation of electrical current in the melt, MHD devices are divided into two main classes: conduction (Fig. 2a) and induction (Fig. 2b). In the first type of devices, electrical current is introduced into the melt directly from the special current leads. The need for contact current supply from the external circuit to high-temperature, chemically aggressive melts restricts the use of such devices in metallurgy. The exceptions are cases when the current in the melt is caused by the process itself (for example, the melting current in the ESR or VAR). These shortcomings are not found in the second type device in which the current in the melt is excited by an induction method with alternating electromagnetic fields (pulsed, running, spinning).

MHD pumps. One of the first effects of the MHD have been used in devices for transporting and dispensing liquid metals (see Figure 2-4). Already in the first descriptions of the electromagnetic pump the most important advantages of these devices are indicated – no mechanical moving parts, the ability to work in a fully enclosed, pressurized volume, smooth control performance.

A large number of MHD pumps with different purpose and design have been developed and are manufactured (Fig. 3) [3, 6, 7]. Their operating principle is based on creating in the channel in the core the difference between the pump pressure through the use of bulk electromagnetic forces. Therefore, in most cases, the flow in the channel is a pressurized pump. In the electromagnetic chute, in contrast to the pump, the melt moves in a free flow, which has a free surface (Fig. 3d).

Electromagnetic pumps are used for handling of magnesium, zinc, tin, lead, gallium, aluminum-based alloys, ferrous metals. Their systems are used in transportation and metering melt into moulds, or moulds for technological or emergency output (drain) from the melt bath tanks, etc. The pumps are manufactured as single units or as part of specialized equipment for heating, furnace

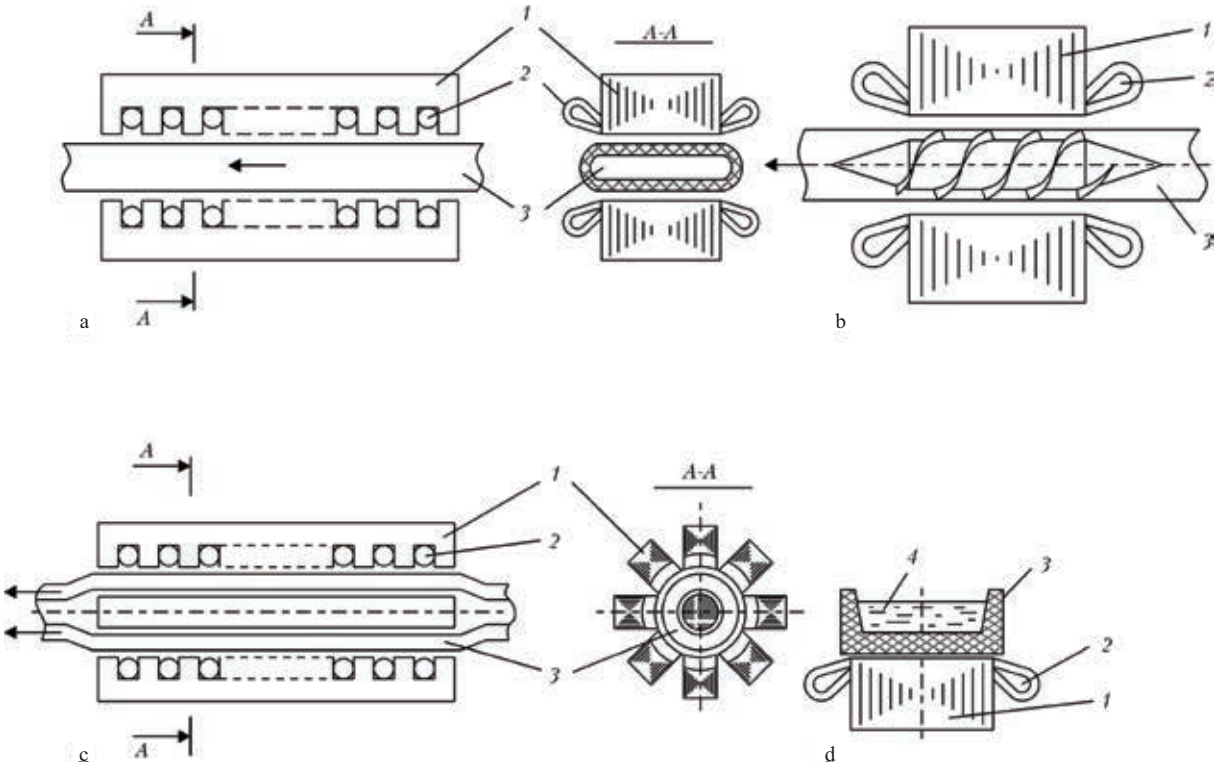

Fig. 3. Induction pumps with a traveling magnetic field (a, c), with a rotating magnetic field and the screw channel (b), electromagnetic trough (g): 1 - magnetic, 2 - winding, 3 - channel; 4 - the liquid metal.

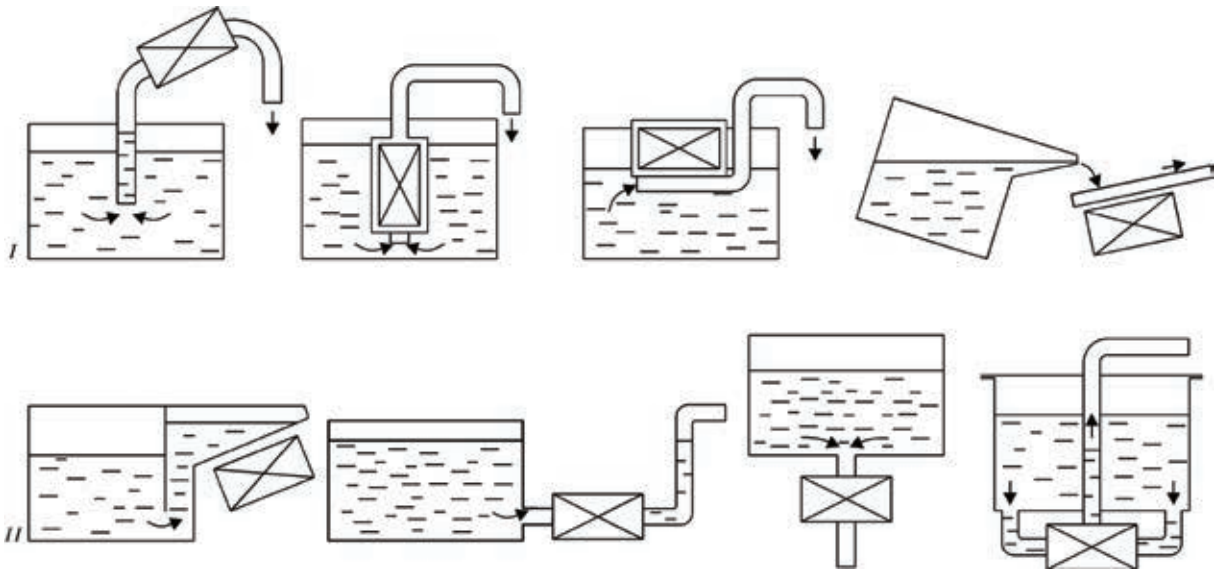

Fig. 4. Schemes of arrangement of electromagnetic pumps, furnaces: I - not associated with the furnace; II - rigidly connected to the furnace.

treatment and casting non-ferrous and ferrous metals (Fig. 4, Table 1). The developed pumps develop the pressure to 6 MPa and performance up to 70 tons of metal per hour power consumption of up to 700 kW [4, 7].

MHD mixers. Another widely used in metallurgy, MHD devices are a class of MHD

Table 1. Characteristics of some commercially available MGD plant [5, 6]

Eqi pment	Metal	Performed operations	Useful melt charge, kg	Supply of alloy in charging, kg/s	
				Minimum	Maximum
MDN-6A-0.16	Al and its alloys	Preheating, ladle treatment and pouring into casting moulds	160	0.3	2.5
MDN-6A-0.25			250	0.4	3.0
MDN-6A-0.4			400	0.5	3.0
MDN-6A-0.6			600	0.6	3.5
99801 MDN-6S)	Lead, tin and their alloys	Melting, preheating, finishing and pouring into casting moulds	600	0.3	3.0
99411 (99412)	Cast iron	Preheating, ladle treatment and casting in centrifugal caousel and automatic moulding lines	2500	0.8	12.0
99413 (MDN-6Ch)	Steel	Induction preheating, storage and periodic supply to solidification mould of eqi pment for electroslag surfacing of rilling rolls	6300	3.0	20.0

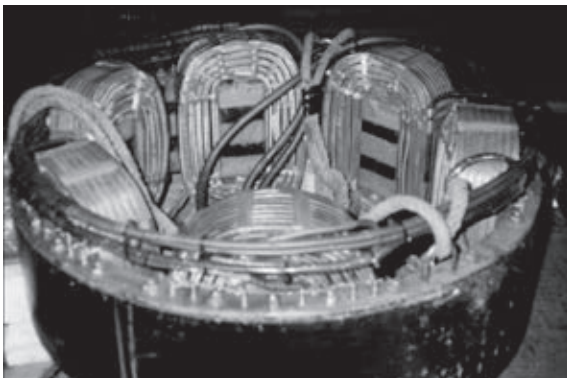

Fig. 5. The appearance of the MHD stirrer with a rotating magnetic field [8].

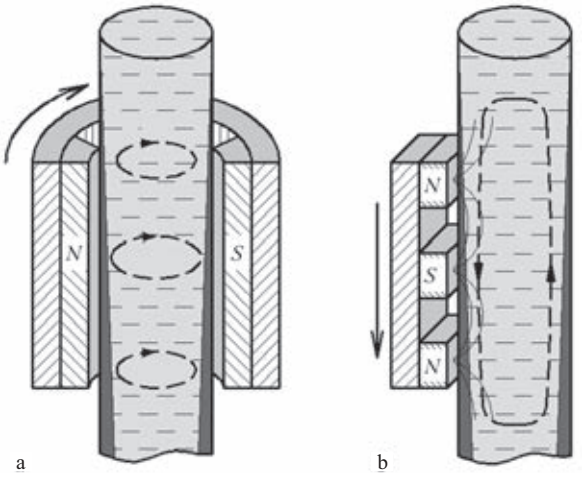

Fig. 6. The scheme of mixing of liquid metal rotating (A) and running (b) magnetic fields.

stirrers.Their operating principle is based on a non-contact exposure they create an alternating magnetic field on the conductive melt. Structurally, the system for electromagnetic stirring has one or more inductors with copper or aluminum windings (Fig. 5). The most commonly used is two- or three-phase alternating current with a frequency of 1... 50 Hz at a power consumption 10...3000 kW. There are two main types of agitator: generating a rotating and traveling magnetic field.

In the first case the electromagnetic stirrer is essentially an induction motor stator (Fig. 5), and the rotor – the liquid metal. Such inductor in the melt creates an azimuthal (around the axis of the bath) rotation (Fig. 6a). The running magnetic field is generated by a plane-linear inductor, creating a melt flow along the poles of the inductor (Fig. 6b). Some modern stirrers used both types of inductors, which allows separate control of the intensity of the azimuthal and meridional flows [9, 10].

In addition to these types of agitator, there are electromagnetic submersible mixers, lowered directly into the melt of the metallurgical furnaces [1]. Their use can reduce the distance between the inductor and liquid metal as the protective lining of the stirrer is much thinner lining furnaces, and thereby increases the

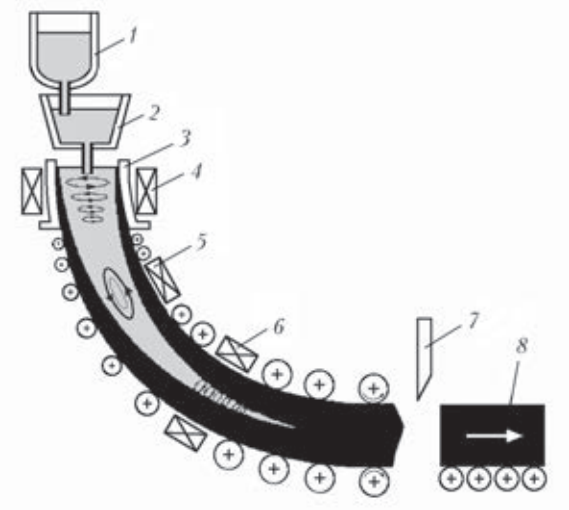

Fig. 7. Electromagnetic stirring in continuous casting of steel: 1 - ladle, 2 - intermediate ladle, 3 - mold; 4-6 - EMS, respectively, in the mold, secondary cooling zone, the zone of the end of solidification, 7 - cutter, 8 - dimensional workpiece.

efficiency of electromagnetic effects.

Continuous casting machine (CCM).Widespread use of electromagnetic stirring (EMS) of the metal obtained by continuous casting of steel billets [3, 10-13]. In this case it is used for the following tasks: improve the internal structure of the workpiece (grinding structure, reducing the degree of segregation, reduction of central porosity); improve the quality of the workpiece surface (reducing the number of surface defects, increasing the thickness of the outer crust); increase the speed of casting metal.

The current CCM use methods of multistage mixing in two or three levels: the mould, secondary cooling zone, the zone of the end of solidification [11] (Fig. 7). In the area of the mould and the end of solidification of continuously cast billet there is equipment, creating a rotating magnetic field, and in the middle of the caster – the running.

EMS in the area of the mould reduces central liquation and porosity of the central zone, improve the chemical homogeneity of the metal, increases heat and reduces probability of breaking a crust of hardened metal, which, in turn, can increase the performance of the casting process.

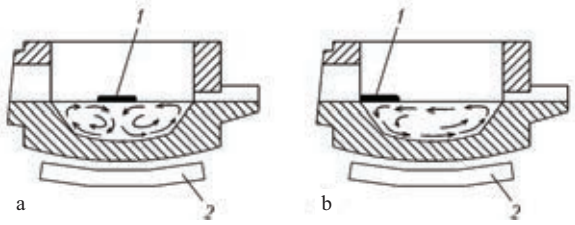

Fig. 8. The movement of the metal and slag in electric arc furnace at different modes of operation of the agitator: a - mixing and b - slag skimming, 1 - slag, 2 - MHD stirrer.

Mixing in the final solidification of billets improves the quality of its central zone, refines the metal structure by inhibiting the growth of columnar crystallization and increases the zone of equiaxial crystals.

In general, the electromagnetic stirring process of continuous casting of steel can result in the following [14]: reduce the number of surface defects 2-3 times; increase the zone of equiaxed crystals 50...100%; reduce the central porosity and liquation to 0 points; increase the casting speed by 20...30%; extend casting with higher superheating temperature for 10...15°C; increase the assortment of pourable grades, including high-carbon and special steels (bearing, stainless and tool).

In addition to the MHD agitator, the use of continuous casting machine with a constant magnetic field reduces the depth of penetration of the jet of metal in the bath (the so-called method of electromagnetic inhibition) [15]. The equipment includes a wall along the magnetizing coils of the mold, creating a strong magnetic field, which slows the rate of entering the jets of metal mould, so that non-metallic inclusions can quickly come to the surface of the meniscus. This prevents the erosion of the narrow faces of the slab crust of the workpiece, decreasing the content of the inclusions and micro-defects in its metal. The use of electromagnetic inhibition provides increased casting speed by 30% without an increase in contamination of the metal inclusions.

Electric arc furnace (EAF). The use of EMF in the EAF allows one to speed up the melting process and improve the quality of the

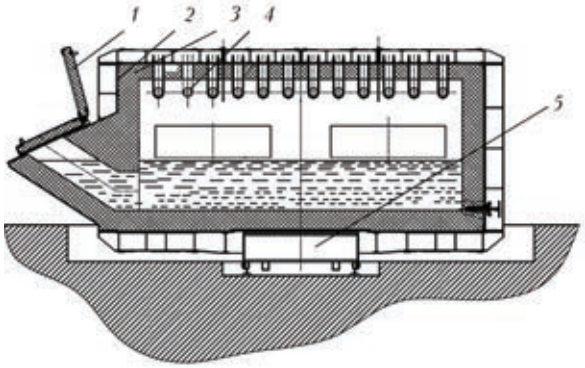

Fig. 9. Chamber electric-mixer type SAMPO: 1 - cover casting 2 - housing 3 - lined 4 - heating elements, 5 - MHD stirrer.

metal [16, 17]. Thus, the temperature gradient along the depth of the EAF bath can reach 100°C, because the arc is directly heated, only in the upper layers of the metal.Mixing equalizes the metal temperature, intensifies the processes of chemical interaction, can distributes the alloying additives.

Electromagnetic effects in the EAF is aimed to perform two basic tasks: mixing of the melt in order to intensify heat and mass transfer, as well as facilitating the process of skimming through the creation of directed motion to the working window of the oven.

The MHD stirrer, which is a detailed stator, is set mostly under the bottom of the furnace (Fig. 8). The windings are fed by currents stirrer speeds ranging from 0.3 to 1.5 Hz, The power per phase reaches up to 860 kV·A [17].

In mixing, the stator windings are switched so that the direction of the magnetic fields at the discharge tip and the working window was opposite (Fig. 8a). This provides an intense vertical mixing of the bath. In the slagging mode the running magnetic field causes the movement of metal from the discharge spout to the working window (Fig. 8b). Slag is also shifted to the working window, making it easy to download through a small slope in the furnace side of the working window.

Technical and economic advantages of using EMF are to increase by an average of 20% furnace productivity, cost of alloying elements, improving the quality of melted metal with a reduction factor of 2-3 marriage to non-metallic inclusions [17].

Preparation and casting of aluminum alloys. Electromagnetic stirring is widely used in the aluminum industry for homogenization and refining of melts in the melting furnace, or handouts, transport ladles, mixers, with semi-continuous casting of ingots [18-21].

In the mixers and ovens set primarily MHD mixers traveling magnetic field, which is placed at the bottom (bottom) mixer or stove, or near the lateral wall (Fig. 9) [18]. These mixers are currently operated at Sayanogorsk, Krasnoyarsk, Bratsk, Novokuznetsk, Irkutsk aluminum plants, the U.S., Canada, France, [19].

The use of EMF allows efficient and lower cost of electricity to bring uniformity to the aluminum alloys in chemical composition. In this case a 25% increase process efficiency by 15%, reduced the amount of electricity consumed and the temperature difference between the mirror and the metal bottoms from 140 to 5...12°C, decreases the saturation of the aluminum melt hydrogen and its oxidation, reduces the amount of slag by 15...25%, and the duration of the preparation of alloys [19].

In semi-continuous casting of aluminum ingot used EMS to a uniform distribution of alloy components in the cross section ingot and control the shape and size of the grains. For intensive mixing of the liquid phase in the solidification of the melt is used MHD mixers that generate flow in horizontal and

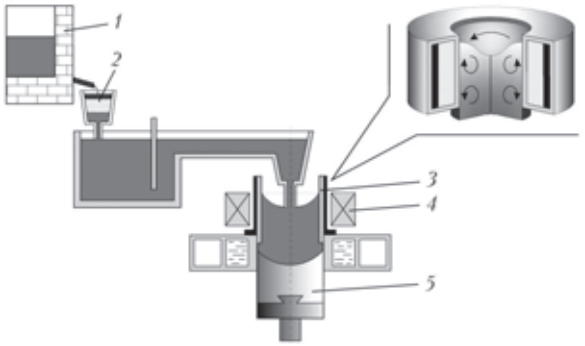

Fig. 10. The scheme of casting aluminum ingots with MHD stirring of the melt: 1 - melting furnace; 2 - filter; 3 - thermal nozzle; 4 - MHD stirrer; 5 - bar.

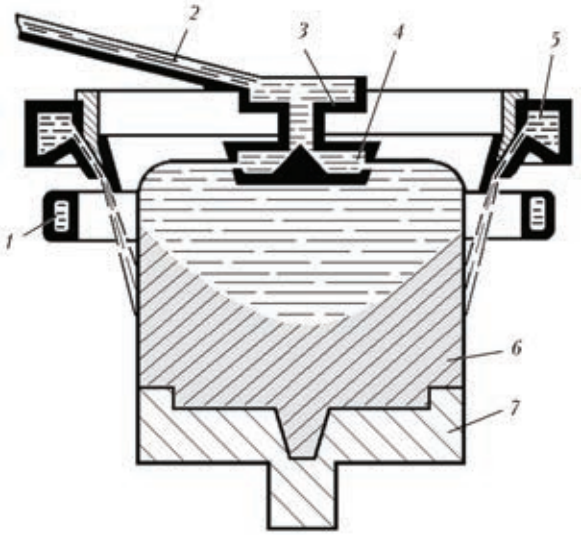

Fig. 11. The scheme of electromagnetic casting in the mould [3]: 1 - inductor; 2 - tray; 3 - junction box; 4 - floating vessel, 5 - the coolant reservoir; 6 - ingot; 7 - base plate.

vertical directions at the same time allow separate control of the intensity of these movements (Fig. 10) [20].

Grinding grain wrought alloys casting with stirring avoids the need to modify their alloys by introducing a responsible use of artificial crystallization centers, which leads to a decrease in values of the resource characteristics of the alloy [20].

Crucibleless melting of metals. A promising direction of MHD effects in metals is the use of electromagnetic forces for the formation of the ingot. An example of such technology is casting in an electromagnetic mould (Fig. 11) [3, 22]. The peculiarity of this process lies in the fact that the purpose of forming non-contact casting pourable metal is fed to the electromagnetic field, confining it to the specified circuits at the same time carry out forced cooling, ensuring the solidification of the casting. This technology is implemented in the casting of aluminum alloys. Technical and economic effects of technology reflected in improving the quality of surface ingots, improving the crystal structure metal, increasing the productivity of the process casting [3, 22].

Another example of the use of electromagnetic force for shaping metal is a crucible

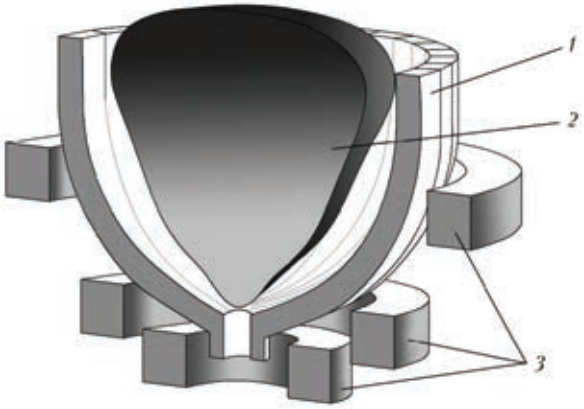

Fig. 12. The scheme of levitation melting in a cold crucible [23]: 1 - a cold crucible (a sectional mold) 2 - the molten metal, 3 - inducer.

(or levitation) fusion [23, 24]. Smelting crucible without contact of the melt with the walls of the crucible is effective in obtaining high-purity metals and alloys (titanium, zirconium, vanadium, tantalum, etc.), when the metal contamination the crucible material is unacceptable.

The principle is based on floating-melting induction heating and electromagnetic levitation (Fig. 12). The inductor formed specially designed high-frequency electromagnetic field induces eddy currents in the metal to ensure its heating and melting.

In turn, the interaction of these currents with stimulating them to contribute to the magnetic field pressed from the wall and holding the melt in a suspended state.

The main drawback of this method of fusion is the limited mass of the melt and its stability during heating. Number of levitating metal can range from several tens to hundreds of grams. Research in this direction is actively developing. For example, in [23] by means of mathematical modeling of the possibility of levitation dvuhkilogrammovogo volume of the liquid metal without contact with the walls of the cold crucible. In the publication [24] is an example of "partial levitation" to 500 kg of molten metal in cold crucible diameter of 600 mm. This process is used when obtaining two-ton ingot of the alloy Ti-6Al-4V (Fig. 13).

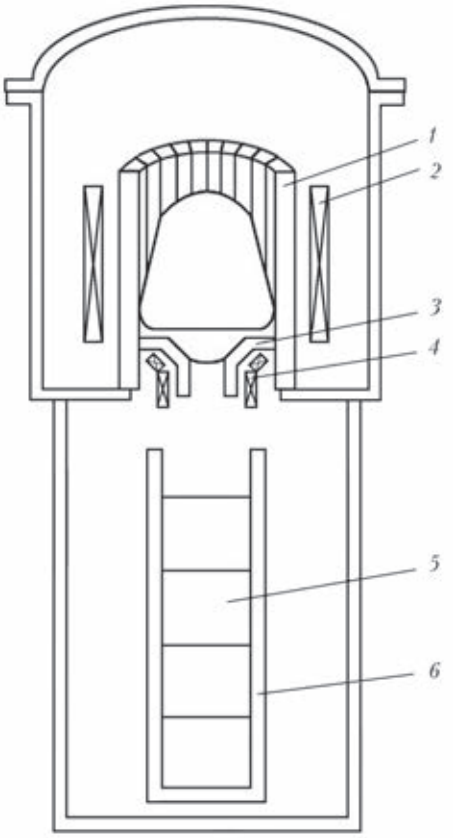

Fig. 13. The scheme of levitation melting in a cold crucible with a bottom release of the metal [24]: 1 - cold crucible (sectional mold) 2 - melting coil, 3 - outlet, 4 - discharge inductor; 5 - bar 6 - mold.

MHD separation. In metallurgical processes MHD separation is used for refining metal from the pores and inclusions, as well as extraction metal from slag [1-3, 25, 26]. There are different mechanisms of MHD separation based on the difference in density and electrical conductivity of materials.

One of the mechanisms of removal of inclusions based on the change in the proportion of melt under the influence of crossed electric and magnetic fields [3]. Thus, an artificial weighting of liquid metal leads to an increase in buoyancy, increase speed and efficiency of non-metallic surfacing inclusions and gas pores. To remove the inclusion of a density higher than that metal, is used to facilitate artificial the melt, contributing to an increase in their rate of deposition on the bottom of the tank or channel.

Another mechanism for the removal of inclusions based on the establishment, under the influence of electromagnetic forces azimuthal rotation of the tub. Inclusions with a density higher than that of the metal under the action of centrifugal forces ousted the walls of the forming device, and the solidification of metal concentrate on the surface of the workpiece.

Table 2. Comparative characteristics of the structure of titanium ingots produced by differentEBM methods [30]

Melting method	Size and typical shape of final β-grains, mm	Size of intragranula α-colonies, μm	Thickness of α-plates in colonies, μm
With EMS of melt	6-7 (size No. 6, eqi axed)	70-100 (size No. 2)	5-7 (size No. 2)
No stirring	7-12 (size No. 9, elliptical)	80-120 (size No. 3)	6-10 (size No. 3)

For different values of electrical conductivity of the melt and the particles suspended in it use of MHD separation based on the force acting on the particle when passing through the melt of an electric current or a magnetic field [27].This principle of separation is used to remove particles such as Cr_3C_2 of copper-based alloys [25] and SiC in aluminum [26], etc.

Electron beam melting (EBM). For electron-beam technology application of electromagnetic effects is crucial, because so far the only way to influence the crystallization process is regulation of the heating surface of the melt in the mold with an electron beam [28].

The use of electromagnetic stirring in the EBL was first implemented in 1970. the Institute of Casting of the NASU [28-30]. Numerous studies conducted in melting of nickel-based alloys, titanium, stainless steels, zirconium, niobium, copper, showed that the use of EMI to reduce specific energy consumption, improve process efficiency, reduce metal loss due to evaporation, to reduce the grain size [30]. An important advantage of EMF in the EBL is the possibility of melting

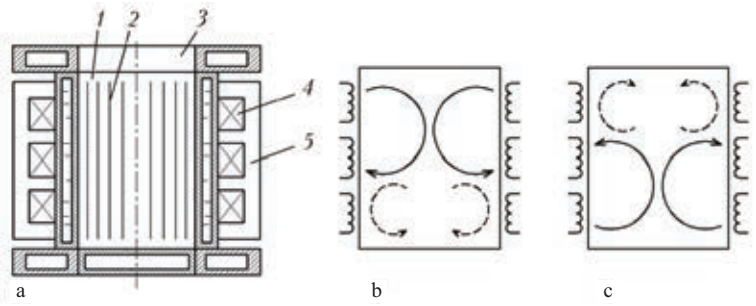

Fig. 14. Diagram of the mold with a system of EMF (a) and the possible paths circulation of the melt (b, c) [28]: 1 - water-cooled copper vessel, 2 - Transverse sections of 3 - water-cooled flange, 4 - inductor coil; 5 - magnetic.

of multicomponent alloys, including those containing volatile elements. To date, have developed different molds with systems EMI, one of which is shown in Fig. 14. Mould is a water-cooled copper cylindrical vessel with longitudinal slits in the area of placement of EMF. It was installed in the casting chamber on the same axis with drain hole melting pot EMS system consists of a coil inductor, located around the tank and covered by a magnetic circuit. Power coils by currents of commercial frequency at a voltage of 18 V and a current of 600 A. Depending on the wiring diagram power system is possible to create EMF circulation of the melt in the mold from the wall to the center (Fig. 14b) and from the center of the wall (Fig. 14, c) or alternately alternating mixing.

In EBM with EMS it is important to minimize the negative effects of electromagnetic fields on the electron beam. The latter is achieved through screening of the magnetic field above the upper water-cooled flange srezomkristallizatora made as a closed loop. The results of evaluating the effectiveness of the use of electromagnetic effects in the melting of titanium ingots VT1-0 are shown in Table 2.

Vacuum arc remelting (VAR). In VAR electromagnetic effects are used for both control the movement of metal, and to stabilize the arc and forced her to move the end face of the consumable electrode [16, 17, 31, 32]. In most cases, the electromagnetic DC solenoid device encircles the mold.

The use of solenoids with axial magnetic field stabilizes the arc and prevents its transfer to the wall of the mold, thus reducing the explosiveness of the furnace.

The results of the use of electromagnetic stirring at VDP for different alloys are different.Mixing a positive effect on the homogenization temperature of the metal and the uniform distribution of alloying components on the volume of the bath, as well as on the structure of titanium alloys [32].

At the same time the azimuthal mixing of the metal can lead to negative consequences, in particular the appearance of spotty liquation. In This applies primarily to the high alloy steels and prone to phase separation (ShKh15, EI437BU, etc.) In this case, take special measures to slow the circulation of the melt. For example, we recommend periodic changes in the polarity of current in the solenoid with a frequency of 0.07 Hz ... 0.017 [17].

In general, the effectiveness of the electromagnetic stirring at VAR is determined in each case for a particular alloy and the size of melted ingot.

Electroslag remelting (ESR). ESR is a favorable metallurgical process in terms of the electromagnetic control [33, 34]. First of all, this is due to the fact that the ESR by molten slag and metal baths runs a significant level of operating current (tens of kA), it can be used for the electromagnetic control. It is also important that the electroslag process is characterized by a wide range of sustainable

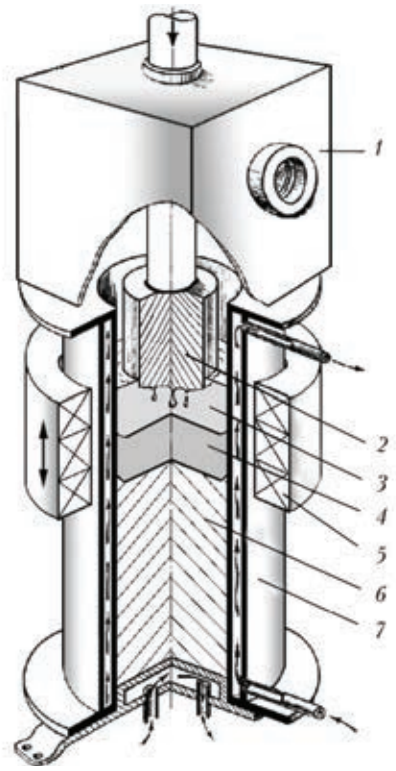

Fig. 15. Scheme of magnetically controlled electroslag melting: 1 - vacuum chamber, 2 - electrodes, 3 - slag bath; 4 - metal bath, 5 - electromagnetic system, 6 - bar; 7 - mold.

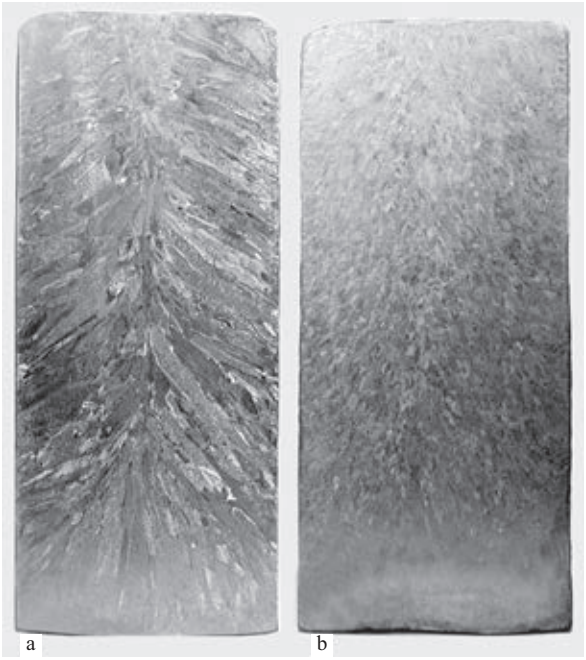

Fig. 16. Macrostructure of titanium ingots ESR, melted without electromagnetic effects (a) and with (b).

modes of its occurrence.

The main objectives of the electromagnetic effects in the ESR is to improve the chemical homogeneity of the melted metal and the improvement of the crystal structure of the ingot.In addition, magnetic fields can affect the especially the melting of the consumable electrode, nature of education and separation of the electrode metal droplets, the trajectories of their motion in the slag bath, and thereby achieve the required technological and metallurgical effects [34].

The principle of electromagnetic interference in ESR is created in conjunction with a special device of an external magnetic field with electric shock melting, resulting in melts formed by three-dimensional electromagnetic forces, leading to a force on the melt.Depending on the characteristics of the external magnetic field in the molten slag and metal Ceska baths, you can create those elektrovihrevye- tion or vibration of the melt.

Already in the first papers on the ESR with the imposition of Magnetic Fields marked refinement of the crystal structure of the ingot, reducing energy consumption and duration of melting [35, 36]. Then it was found that the steady rotation about the axis of the melt bath, due to the superposition of longitudinal and radial magnetic fields can cause adverse effects - increasing the depth of the metal bath and undesirable changes in its shape [37].

In [34, 38, 39] studied the effect of external magnetic fields on the technological and ESR characteristics of titanium steel alloys. Based on these studies the technology of magnetically controlled electroslag melting (MEM) of titanium alloys (Fig. 15).

It is shown that an effective scheme of the electromagnetic interference in MEM is a pulsed effect on steel bath longitudinal magnetic field. In this case, the magnetic field interacts with the radial component of the current heat. This scheme allows for the bath as elektrovihrevye flow and vibration of the melt. This ensures intensive mixing of the liquid metal and grinding of the crystal

structure of the ingot (Fig. 16). The formation of homogeneous fine-grained structure for high manufacturability of metal on the stage of the deformation and subsequent redistribution, the high value of its mechanical properties and performance.

Conclusion

MHD technology are increasingly practical application in various metallurgical processes. In addition to technological solutions problems of transportation and dispensing molten metal and slag, the impact of external magnetic fields are widely used to intensify heat and mass transfer in melting units and manage the process of crystallization of the metal. Application of MHD effects in the industry aimed at improving the properties of metals and alloys produced, reducing their cost, to obtain new properties and materials.

References

1. Verte L.A., Magnetohydrodynamics in Metallurgy. - Moscow: Metallurgiya, 1975. - 288.
2. Povkh IL, Cole, AB, Chekin BV Magnetohydrodynamics in Metallurgy. - Moscow: Metallurgiya, 1974. - 240 s.
3. Verte L.A., MHD technology in the production of ferrous metals. - Moscow: Metallurgiya, 1990. - 120 p.
4. Povkh I., Barinberg A., B. Barinberg Professions of magnetic hydrodynamics / / Nauka i Zizn' - 1977. - № 6. - Pp. 40-46.
5. Dubodelov V.I., Status and prospects of research and development in the field of metallurgical MHD / / Prots. Lit'ya. - 1998. - Number 3. - S. 36-43.
6. Magnetodynamic pumps for liquid metals / VP Polischuk, M. R. Ching, R. K. Horn, and others - Kiev: Naukova. Dumka, 1989. - 256 p.
7. http://www.niikhemz.com.ua/24.htm.
8. Barglik J., Smagor A. Some aspects of electromagnetic stirring during process of continual steel casting / / Proc. of the 6th Intern. conf. on Electromagnetic processing of materials EMP 2009 (Oct. 19-23, 2009, Dresden, Germany). - Dresden, 2009. - P. 684-687.
9. MULTIMAG - A MULTIpurpose MAGnetic field system for EMP / A. Cramer, J. Pal, Th. Gundrum, G. Gerdeth / / Ibid. - Dresden, 2009. - P. 826-829.
10. http://www.icmm.ru/ ~ lab4/download/mhdadvert.htm.
11. The use of electromagnetic stirring in continuous casting technology / I. Shifrin, VG Grachev, VI Plantus, etc. / / Steel. - 2005. - Number 1. - S. 17-20.
12. Kudrin V.A., Furnace treatment of iron and steel. - Moscow: Metallurgiya, 1992. - 336.
13. Thomas B., Chaudhary R. State of Art in Electromagnetic Flow Control in Continuous Casting of Steel Slabs / / Proc. of the 6th Intern. conf. Electromagnetic processing of materials EMP 2009 (Oct. 19-23, 2009, Dresden, Germany). - Dresden, 2009. - P. 9-14.
14. http://www.vniimetmash.ru/products/mnlz/mnlz.shtml.
15. Kollberg S. Continuous Cast Proc. 4 th Intern. Iron and steel Congr. (London, 12-14 May, 1982). - London, 1982. - B5/1-B5/4.
16. Electrical Industrial Furnaces: Arc furnace and install special heating / A.D. Svenchanski, - Moscow: Energoatomizdat, 1981. - 296.
17. Tyre, L.L, M. J. Electromagnetic devices for controlling the circulation of the melt in the electric furnaces. - Moscow: Metallurgiya, 1975. - 224.
18. Babyshkin G.A, Wood, A.A., Lazarev V.A., Chamber electric-mixers for the aluminum industry / / www.therm.ru/60/60.files/60-11.htm.
19. http://www.npcmgd.ru/ ("Research and Production Center MHD").
20. Borisov, V.G., Met. Mashnistoeniya,- 2009. - № 3. - S. 39-44.
21. Kim M., Kim J., Park J. Designing of Continuous Casting Machine for Near Net Shape Aluminium / / Proc. of the 6th Intern. conf. Electromagnetic processing of materials EMP 2009 (Oct. 19-23, 2009, Dresden, Germany). - Dresden, 2009. - P. 323-325.
22. Mochalov P.P., Getselev Z.N., Continuous casting ingot with the formation of an electromagnetic field / / Tsvetn.. Metally. - 1970. - № 8. - S. 62-63.
23. Bojarevics V., Roy A., Pericleous K. A. Magnetic Levitation of Large Liquid Volume / / Proc. of the 6th Intern. Scientific Colloquium «Modelling for Material Processing» (Riga, Sept. 16-17, 2010). - Rigam, 2010. - P. 15-20.
24. Okumura T., Yamamoto K., Shibata M., Large Scale Cold Crucible Levitation Melting Furnace with Bottom Taping Nozzle / / Proc. of the 6th Intern. conf. Electromagnetic proc. of materials EMP 2009 (Oct. 19-23, 2009, Dresden, Germany). - Dresden, 2009. - P. 521-524.
25. Electromagnetic separation of inclusions from molten copper by alternating electromagnetic field / M. Higuchi, H. Ambai, S. Shimasaki at al. / / Proc. of the 6th Intern. conf. on Electromagnetic proc. of materials EMP 2009 (Oct. 19-23, 2009, Dresden, Germany). - Dresden, 2010. - P. 86-89.
26. Taniguchi S., Yoshikawa N., Takahashi K. Application of EMP to the separation of inclusion particles from liquid metal / / Proc. of the Joint 15th Riga and 6th PAMIR Intern. conf. «Fundamental and Applied MHD» (Riga, June 27-July 1, 2005). - Rige, 2005. - P. 55-63.
27. Electric eddy flows / V.V. Boyarevich, J. J. Freiberg. - Riga: Zinatne, 1985. - 315 p.
28. Ladokhin S.V., Cherniavsky, V.B., Gladkov, A.S., An experimental study of the distribution of electromagnetic fields in the mold to produce ingots Electron Beam plants / / Prots. Lit'ya, 2006. - № 1. - p. 17-22.
29. Panasyuk, L.S., Ulyanov, V.L., Yaavich V.E., Electromagnetic stirring of liquid metal in electron-beam melting / / Casting of refractory metals. - Kiev: IPL AN USSR, 1970. - Issue 1. - S. 76-87.
30. Cherniavsky, VB, Ladokhin SV, Gladkov, A. / / Prots. Lit'ya, - 2005. - Number 1. - S. 48-55.
31. Effect of electromagnetic stirring on melt pool free surface dynamics during vacuum arc remelting / P. Chapelle, A. Jardy, J. Bellot, M. Minvielle. / / J. of Materials Science. - 2008. - V. 43. - P. 5734-5746.
32. Effects of VAR Processing Parameters on Solidification Behavior of Ti-10V-2Fe-3Al Alloy Ingot / Yang Zhijun, Kou Hongchao, Chang Hui at al. / / Special Casting & Nonferrous Alloys. - 2010. - № 4. - P. 295-297.
33. Kompan Ya.Yu, Shcherbinin E.V., Electroslag welding and melting with controlled MHD processes. - M.:

Mashinostroenie, 1989. - 272.
34. Protokovilov I.V. Magnetically controlled electroslag melting of multicomponent Ti alloys, Dissertation, National Academy of Sciences of Ukraine, Kiev 2006. - 178 p.
35. Dudko D.A., Rublevsky I., Electromagnetic mixing of slag and metal bath in electroslag process / / Avt. Svarka - 1960. - Number 9. - S. 12-16.
36. Trochun I.P., Chernysh V.P., Magnetic Control crystallization at ESR / / Svar. Proiz., - 1965. - Number 11. - S. 3-5.
37. Research and development of methods for controlling the structure of the crystallizing ingot by applying ESR magnetic field / Paton, BER., et al., Probl. spets. elektromet., - 1989. - № 4. - S. 3-7.
38. Kompan Ya.Yu., et al., On the intensification of electromagnetic interference in magnetically electroslag melting of titanium alloys / / Sovremen. Elektromet., - In 2007. - № 4. - S. 3-7.
39. Kompan Ya. Yu, et al., Magnetically electroslag melting (MEM) of titanium alloys with discrete effects of magnetic fields / / Proceedings of the Intl. conference. «Ti-2008 in the CIS" (18-21 May 2008, St. Petersburg). - St. Petersburg, 2008. - SA 96-9 .

Submitted 12.7.2011

Advances in Electrometallurgy 2011 **9** *(4) 251–254*
Translated from Sovremennaya Elektrometallurgiya 2011 **9** *(4) 42–45*

ENERGY AND RESOURCES SAVING

Electrothermal compacting of metallic materials

V.A. Shapovalov, F.K. Biktagirov, V.R. Burnashev, V.I. Kolesnichenko, V.V. Stepanenko, N.V. Reida, O.V. Karuskevich and D.V. Botvinko

EO .P aton Electric Weld ng Institute,K iev

Brief analysis of process flow charts of producing a pressed billet of non-compact charge for next remelting is given. Shown are the challenges and economic rationality of pressing the non-compact charge by combination of processes of electric heating and negligible forces of pressing without application of powerful and expensive press equipment. The design of a pilot installation is described, successive operational flow chart of pressing the non-compact charge and main technological parameters of the process are given.

The development of new energy-saving and cheap technologies, and also of the appropriate equipment for the close production of metallic materials is a very important task.

Regardless of the relatively high level of the production of metal products, and the process of production is accompanied by the formation and buildup of a large amount of waste. This is determined both by the special features of the technology and the technical requirements on completed products. Taking into account the fact that a metallic fond of approximately 40,000,000,000 t has been formed in the last 40 years, it is easy to imagine the scale of buildup of secondary resources which must be directed to metal circulation. In particular, this applies mainly to expensive high reactivity and refractory metals (titanium, zirconium, niobium, etc).

For example, in processing of titanium by cutting, up to 40% of metal is transferred into shavings, and in the production of titanium castings the yield of material suitable for components for important applications is only 20-25% [1]. Recently, after the worldwide economic crisis, the interest in titanium has been renewed. This material is characterised by a set of unique properties which makes it almost irreplaceable in various strategically important areas such as the petrochemical, aerospace, chemical, etc. The country producing (and Ukraine is such a country) but not using titanium converts this into the raw material allowance when the titanium page has not yet started there.

Basically, in the bulk of the waste (and not only titanium waste) is a conditional material which should be returned into production

for optimisation and appropriate reduction of the production costs of complete products, thus completely closing the metal circulation circuit.

It should be mentioned that a certain part of the waste, especially large piece waste, is used directly in melting system without preliminary processing. However, there is a large range of metallic materials (shavings, cuttings, wire, granulated powder, sponge, etc) which can be used without preliminary compacting or, at least, we use is greatly complicated and requires quite expensive additional technological operations.

Therefore the problem of compacting these materials to ensure the maximum utilisation in the metal circulation circuit is of primary importance and the need for solving this problem is economically justified and efficient. In addition, another important problem of compact transport of these materials to the area of further processing and rational loading into the melting systems will also be solved.

However, regardless of the abundance of the new methods of compacting of metallic materials (cold pressing, sintering, stamping, electric pulse briquetting, etc) they cannot ensure, because of a number of technical and economic reasons, the formation of high-quality, large and cheap compacted blanks suitable for further use in the metal circulation system [3-6].

In the group of the main shortcomings it is important to mention the following: restricted length of the blank produced in pressing into a dead-end die, low density of the briquette in electric pulse compacting, insufficient strength, the presence of cracks and curvature of the blanks in cold pressing. In addition to this, to produce large blanks by the method of cold pressing, it is necessary to generate a very high mechanical forces with the specific compacting pressure greater then 500 MPa, i.e., use large and expensive equipment (US$10 million).

Taking into account the current situation, the E.O. Paton Electric Welding Institute, Kiev has attempted to solve this problem and this has resulted in the develop meant of a unique, highly efficient technology of compacting metallic materials based on combining the process of pressing and electrothermal heating. This combination increases the plasticity of the material compacted in a special dye and greatly reduces (halves) the pressing force. A number of technological operations, characteristic of the conventional pressing matters (vacuum annealing, welding, etc) are omitted and the quality of produced blanks is improved.

The advantages of the proposed technology, in comparison with the foreign analogues, include the possibility of producing long and large blanks because the process is realised in a continuous die with the current supplied directly to the shaping blank which in turn reduces the electrical consumption, improves the efficiency and, correspondingly, the productivity of the compacting process.

The process is realised in the portional manner in the semi-continuous regime, and each portion is heated in two stages: in the first stage - to the desorption temperature of the gas and rare-phase contaminants, in the second stage to the temperature of hot deformation of the processed material. This increases the quality of components and the efficiency of compacting.

The technology is especially efficient for compacting expensive metals and alloys with high strength and elasticity modulus values. This is out in the formation of both solid and hello blanks which can subsequently be used in the compacted form as remelting electrodes, master alloys, deoxidation agents, etc in any melting systems.

The proposed technology was developed in experimental equipment specially developed for this purpose, Fig. 1. The optimum technological parameters of compacting of different metallic materials (steels, cast iron, aluminium, creep-resisting alloys, titanium, etc), differing in the physical properties (specific the race, heat and electrical conductivity) were determined [6-8]. The materials of different sizes and grain size composition were used.

Figure 2 shows the general view of the combined blank compacted from the titanium

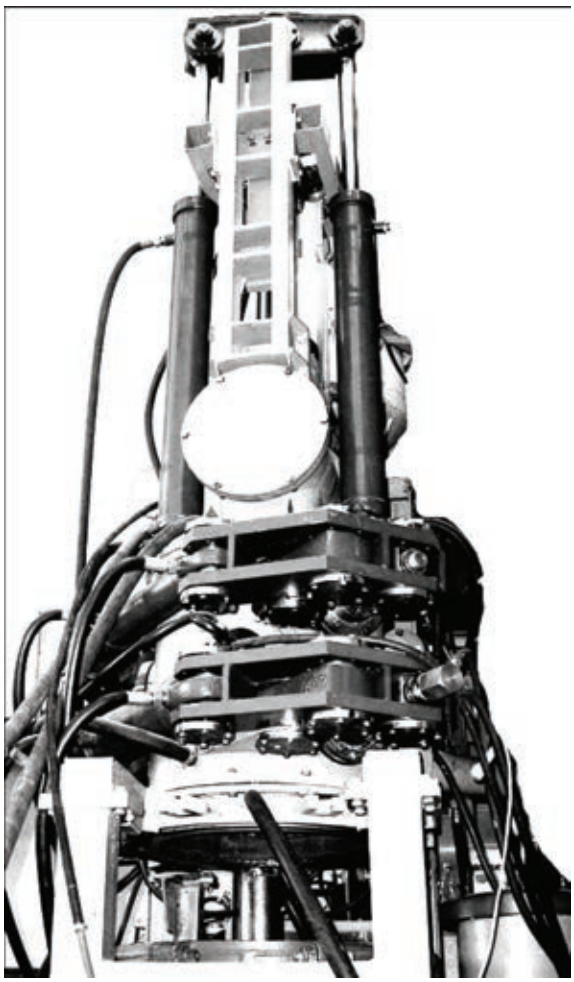

Fig. 1. The general view experimental equipment for compacting metallic materials.

Fig. 2. A blank produced from titanium shavings of different types.

shavings of different types and dimensions, and Fig. 3 shows four different blanks, produced from three fractions of titanium sponge: 2-5; 5-12 and 10-30 mm. Figure 4 shows the blanks of fine (ShKh16GS steel) and large

Fig. 3. Blanks compacted from Ti sponge of different fractions.

Fig. 4. Blank compacted from 100% fine steel shavings of SkKh15SG steel (a) and the large shavings of EP609-Sh creep resisting alloy (b).

shavings of EP609-Sh creep-resisting alloy.

In the experiments, it was shown that the resultant blanks are very strong, as confirmed by the effect of impact loading of 6.5–7.0 MPa on the specimens, the density of the blanks was 70–75% of the theoretical value (density of monolithic metal), which is sufficient for use as consumable blanks in further remelting.

The experiment shows that with the reduction of the grain size composition of the metallic material, the density of the compacted blanks increases. This is explained by the presence of a large number of contact point between the fine particles and, consequently, the more efficient heating in local melting in the compacting process. With increase of the size of the fractions it is necessary to

Table 1. Technical characteristics of equipment for electrothermal compacting

Compacted material	titanium, zirconium, steel, creep resisting alloys
Type of charge	shavings, sponge, powder, cuttings
Size of compacted blanks (electrodes), mm:	
diameter	200, 500
length	3000
Density of produced blanks, % in relation to theoretical density (density of monolithic metal)	70-75
Current density, A/mm^2	1.5
Specific energy consumption, kW h/kg	0.8-1.2
Dosing and supply of compacted material into die	cartridge supply from a cell bunker
Atmosphere in compacting	neutral (argon) vacuum, air
Consumption of cooling water, m^3/h	20
Pressure of cooling water, MPa	0.4
Productivity of eqi pment t, year	3000

slightly increase the level of supplied current and heating time of each portion to produce the guaranteed a high-density structure.

In the process of mastering technology it was necessary to overcome a number of difficulties which required both design and technological approach. For example, it was important to eliminate problems with the supply of large (without preliminary refining) and twisted shavings into the compacting zone, improves the electrical circuit (the presence of a single heat source resulted in a slight asymmetry of compacting), minimise the probability of formation of electric arc discharge in the conditions of mobile current supply to the blank being shaped (compacted), etc.

The resultant experience and determine the relationships obtained in the experiments in experimental equipment enabled the development of more efficient high productivity pilot plant equipment for compacting high-quality and economically efficient long blanks with the stable physical–mechanical properties throughout the entire cross-section using different metallic materials, such as shavings, sponge, powder, granules, cutoff pieces, etc.

In conclusion, it should be stressed that the industrial application of the proposed technology and of appropriate equipment should make it possible to develop a closed (complete) cycle of returning expensive secondary resources into production. This is especially important for large metallurgical and engineering plants. The recovery time of equipment is 8-12 months, depending on the cost of compacted materials.

References

1. Paton, B.E., et al., Spets. Elektrometall, 1974, No. 24, 96-102.
2. Pol'kin, I.S., Promising directions of investigations in the area of production and application of titanium alloys Ti-2005 in the CIS countries, Kiev, 2005, 20-30.
3. Anoshkin, N.F., et al., The melting and casting of titanium alloys, Metallurgiya, Moscow, 1970s.
4. Nikol'skii, L.A., et al., Hot stamping and pressing of titanium alloys, Mashinostroenie, Moscow, 1975.
5. Abramova, K.B., et al., Tsvetn. Metally, 1996, No. 12, 70–74.
6. Zhadkevich, M.L., et al., Sovremennaya Elektrometallurgiya, 2005, No. 3, 64–67.
7. Shapovalov, V.A., et al., Sovremennaya Elektrometallurgiya, 2009, No. 3, 43–45.
8. Paton, B.E., Patent 7997, Ukraine, MPC C 20 2B/1/248, A method of compacting metallic charge, published August 10, 2007, Bulletin No. 12.

Submitted 23.9.2011

Advances in Electrometallurgy 2011 **9** *(4) 255–258*
Translated from Sovremennaya Elektrometallurgiya 2011 **9** *(4) 45–48*

Electroslag remelting of electrodes compacted from the shavings of austenitic stainless steels

V.A. Shapovalov, V.R. Burnashev, F.K. Biktagirov, A.P. Ignatov, G.F. Myal'nitsa, V.V. Stepanenko, M.A. Bragin, V.N. Pudikov, D.V. Pod'yachev, D.V. Botvinko, D.M. Zhirov and A.V. Gnatushenko

EO .P aton Electric Weld ng Institute,K iev

Optimum technological parameters of compacting the austenite stainless chips into electrodes for ESR are defined. The dependence of electrode density on granulometric composition of chips was established. The optimum conditions of ESR of pressed electrodes were found. The quality of obtained method was studied.

The austenitic 18-10 steels are used widely in the group of stainless steels. Evaluating the energy consumption of production of austenitic stainless steels throughout the entire life-cycle, the authors of [1] concluded that when using the initial materials with the production volume of 17 million t/year without addition of the secondary materials, it is necessary to use $9 \cdot 10^{17}$ J of primary energy, resulting in the emission of 61 million t of CO. Partial application of waste material in the melting of steel reduces the energy consumption by 33% (to $4.4 \cdot 10^{17}$ J) in the emission of CO by 32% (to 29 million t). However, if the steel is produced using only the scrap, the energy requirement decreases by 67% and the CO emission by 70%.

This shows that processing of the waste of stainless steel is not only economically efficient but also ecologically effective. The processing of shavings is the most complicated part of this process. Remelting of the shavings requires preliminary compacting both to reduce the degree of burnout and irreversible losses and also to facilitate transport and loading into the melting system.

There are various methods of compacting metals (hydrostatic cold electric pulse pressing, explosion compacting, sintering, stamping and rolling) which, however, do not make it possible to prepare efficiently the processing of shavings of high-alloy steels and alloys, including stainless steels [2, 3].

The E.O. Paton Electric Welding Institute, Kiev has developed a method and constructed pilot plant equipment for the compacting of shavings by the method of semi-continuous hot pressing [4–6]. Experiments with the pressing of various materials (titanium sponge, shavings of EP-609 steel, cast iron, aluminium, etc) shows the promising nature of utilisation of the metallic waste by this method.

The advantage of the proposed method of compacting the charter undercurrent is, in addition to the possibility of producing long blanks, the burnout from the shavings of remnants of the lubricating–cooling liquid (LCL) in loading the material to be compacted to high temperatures. Consequently, the shavings can be used without preliminary cleaning to remove organic remnants from machining.

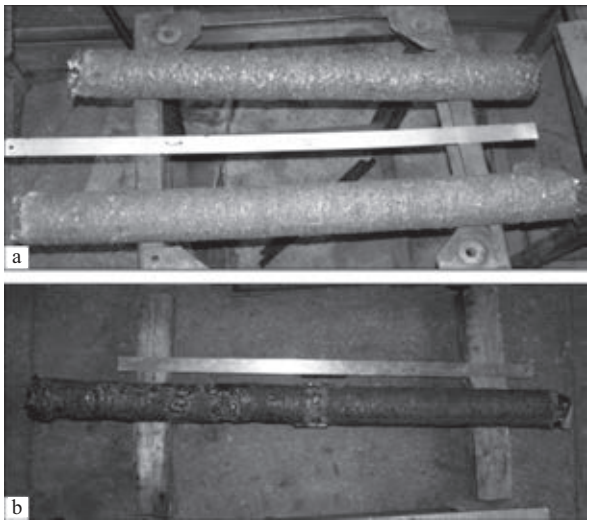

Fig. 1. The produced electrodes: a) compacted (L = 1000 mm); b) assembled from two pressings (L = 1880 mm).

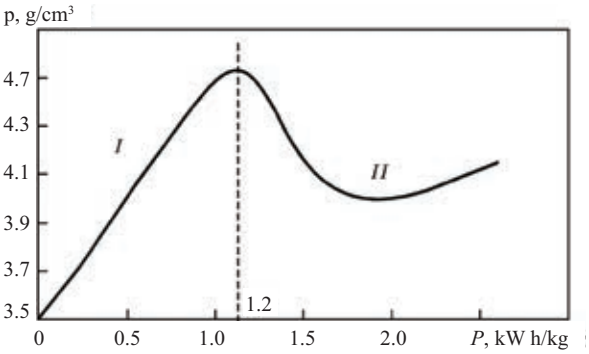

Fig. 2. Dependence of density of the compacted blank on the specific consumption of electric energy P: I) copper shavings 10–25 mm; II) large shavings, 25–70 mm.

Fig. 3. Electroslag remelting of compacted electrodes.

The shavings of a mixture of austenitic steels of type Cr18Ni9 and Cr18NiTi was supplied by the company Zorya-Mashproekt (Nikolaev). After crushing, the charge was not rinsed to remove the remnants of the LCL, and was subjected to compacting to blanks 100 mm in diameter and up to 1000 mm long. The pressing conditions: electric current, passed through the charge, 10–12 kA, applied voltage 12–17 V. The mass of the single portion of the shavings, loaded into the die of pressing equipment, was 650 g, pressing time 3 s, specific consumption of electric energy 0.5–1.0 kW·h/kg.

The individual portions of the shavings were heated to the softening temperature during compacting and in areas they were heated to the liquid–solid-state and efficiently bonded together at a pressing pressure of up to 2.5 MPa. This resulted in the formation of long welded-pressed blanks used as the consumable electrode in electroslag remelting. If necessary, the blanks were welded together by manual welding to produce a consumable electrode for electroslag welding up to 1800 mm long (Fig. 1).

The density of the electrodes of the stainless steel, compacted from the shavings, varied in the range 3.9–4.75 kg/cm^3, which was equal to 54–64% of the density of cast metal. The density of the compacted metal depend strongly on the degree of refining of the shavings. In compacting finer shavings, the density is higher (Fig. 2). The graph shows that for the shavings with the size of 10–25 mm, the optimum consumption of electric energy for pressing is approximately 0.5–0.7 kW·h/kg. A further increase of pressing current

Table 1. Chemical composition of melted stainless steel

Ingot No.	Mass fraction of elements, %						Gas content, %		
	Ni	Cr	Ti	Si	Mo	C	[O]	[N]	[H]
1	9.8	17.0	0.3	0.67	1.3	0.11	0.016	0.049	0.0003
2	10.0	18.5	0.99	0.63	1.4	0.12	0.013	0.42	0.0003
3	10.4	18.4	0.24	0.61	0.57	0.15	0.016	0.039	-0.0004
GOST 977-98	8-11	17-20	5C-07	-	≤ 2.0	≤ 0.12	-	-	

Fig. 4. External appearance of a pilot planned batch of billets of stainless steel melted from compacted electrodes.

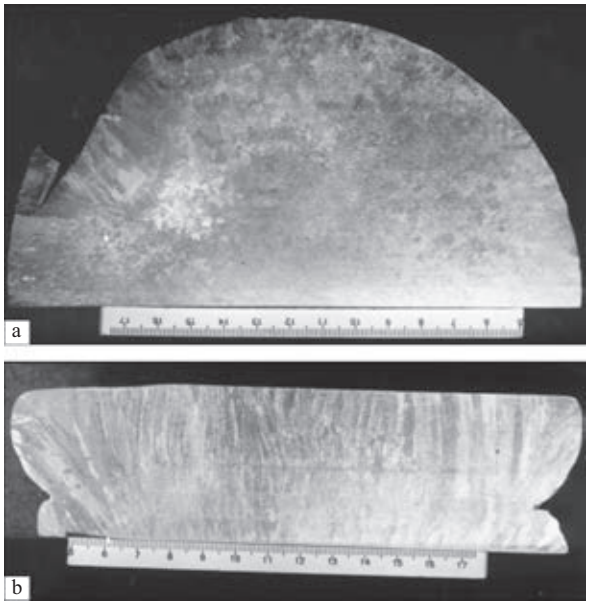

Fig. 5. Macrostructure of the transverse (a) and longitudinal sections (b) of the billets of ESR stainless steel.

and time is not efficient from the economic viewpoint.

The shavings of the stainless steels, compacted into the electrodes, were remelted by ESR in a solidification mould 175 mm in diameter. Melting was carried out by two methods: in a dead end solidification mould and with withdrawal of the billets from the solidification mould.

ESR was carried out using ANF-6 slags and a mixture of slags ANF-6 and AN-295 at the ratio of 1:2 and the following conditions were used: I = 2.0–3.5 kA, U = 37–47 V (Fig. 3). The productivity of the melting was 1.3–1.9 kg/min.

Remelting resulted in the formation of a pilot planned batch of billets with the total weight of 350 kg (Fig. 4). The mass of the billets varied from 35 (melting in the dead-end solidification mould) to 62 kg (with withdrawal of the billets).

Specimens were taken from the produced billets to determine the quality of produced metal and the chemical composition and carry out metallographic analysis.

Table 1 shows that the content of the elements in the remelted metal deviates from the chemical composition of 12Cr18Ni9Ti steel with respect to carbon and titanium. This is associated with the fact that processing was carried out using a mixture of shavings of

Table 2. Mechanical properties of the metal of billets of 12Cr18Ni9Ti stainless steel

Metal	MPa		%		KCU, kJ/m^2
Melted from shavings	229.1	468.7	50.9	64.3	800
Reqi rements of GOST 977-88	≥ 196	≥ 441	≥ 25	U32	U590

titanium containing steel Cr18Ni10Ti and titanium-free steel 12Cr18Ni9. Metallographic studies of the templates, taken from the bottom (Fig. 5a) and central (Fig. 5b) parts of the billets shows that the metal is dense, without visible defects.

The mechanical tests of the specimens of the steel shows that the properties of the steel satisfy the requirements of GOST 977-80 standard (Table 2).

On the basis of the experimental results it can be concluded that the processing of the shavings by pressing into a consumable electrode followed by electroslag remelting of the electrode produces, from 100% shavings, high quality metal and the proposed method is an efficient resources saving technology.

Conclusions

1. The investigations of compacting of the stainless steel shavings show that the method of electric heating of the charge with simultaneous pressing is an efficient method of producing long electrodes.

2. The optimum technological parameters of compacting the shavings have been determined.

3. The electrodes with a diameter of 100 mm, up to 1800 mm long were produced from stainless steel for subsequently melting by the ESR method.

4. The experimental results also show that the density of the electrode depends on the grain size composition of the shavings (as the shavings become finer, the density of the electrode improves).

5. The optimum parameters of the ESR of produced electrodes have been determined. The quality of molten metal has been determined.

References

1. Jeremiah, J., et al., In: Proceedings of the conference: Metallurgy. Energy methods of processing stainless steel, 2009, No. 1, 50B10.
2. Abramova, K.B. and Samuilov, S.D., Rynok vtorychnykh metallov, 2005, No. 2, 50–54.
3. Stepanov, S.I., Investigation of the process of hot pressing and properties of steels produced from steel shavings, Dissertation, Kiev, 1967.
4. Zhadkevich, M.L., et al., Sovremennaya Elektrometallurgiya, 2005, No. 3, 64–67.
5. Paton, B.E., et al., Patent 7997, Ukrain, MPK S22 V1, Method of compacting metallic charge, 10.8.2007, Bull. No. 12.
6. Shapovalov, V.A., et al., Sovremennaya Elektrometallurgiya, 2009, No. 3, 43–45.

Submitted 23.9.2011.